

Ecological Invasion, Roughened Fronts, and a Competitor's Extreme Advance: Integrating Stochastic Spatial-Growth Models

Lauren O'Malley^{a,c}, G. Korniss^a, Thomas Caraco^{b,*}

^a*Department of Physics, Applied Physics, and Astronomy, Rensselaer Polytechnic Institute, 110 8th Street, Troy, NY 12180-3590, USA*

^b*Department of Biological Sciences, University at Albany, Albany, NY 12222, USA*

^c*Current address: Department of Mechanical Engineering, Boston University, 15 Saint Mary's Street, Brookline, MA 02446, USA*

Received: 17 January 2008 / Accepted: 15 January 2009 / Published online: 14 February 2009

© Society for Mathematical Biology 2009

Abstract Both community ecology and conservation biology seek further understanding of factors governing the advance of an invasive species. We model biological invasion as an individual-based, stochastic process on a two-dimensional landscape. An ecologically superior invader and a resident species compete for space preemptively. Our general model includes the basic contact process and a variant of the Eden model as special cases. We employ the concept of a “roughened” front to quantify effects of discreteness and stochasticity on invasion; we emphasize the probability distribution of the front-runner's relative position. That is, we analyze the location of the most advanced invader as the extreme deviation about the front's mean position. We find that a class of models with different assumptions about neighborhood interactions exhibits universal characteristics. That is, key features of the invasion dynamics span a class of models, independently of locally detailed demographic rules. Our results integrate theories of invasive spatial growth and generate novel hypotheses linking habitat or landscape size (length of the invading front) to invasion velocity, and to the relative position of the most advanced invader.

Keywords Ecological invasion · Front-runner distribution · Extreme-value statistics · Preemptive competition · Spatial model · Stochastic roughening

1. Introduction

Invasive species threaten biodiversity in many ecological communities (Ruesink et al., 1995; Rosenzweig, 2001), and impose significant costs on agriculture and public health

*Corresponding author.

E-mail addresses: lomalley@bu.edu (Lauren O'Malley), korniss@rpi.edu (G. Korniss), caraco@albany.edu (Thomas Caraco).

(Pimentel et al., 2000). Spatial advance is the most obvious phase of invasion (Shigesada and Kawasaki, 1997; Hastings et al., 2005), and perhaps the most important (Lockwood et al., 2007). Indeed, the dynamics of advancing fronts challenges our capacity to predict how invasive species, emerging infections, and evolutionary adaptations spread across landscapes (Andow et al., 1990; O'Malley et al., 2006a). Our study emphasizes certain essential features, signature characteristics, of advancing fronts that let us integrate some common models of stochastic spatial growth.

We model preemptive competition between an invader and a resident species as a stochastic process in a two-dimensional environment. As the invading competitor advances, the model exhibits variability of the invader's location about the front's mean position. Generation of variability along the front separating invader and resident species is called interface roughening (Krug and Meakin, 1990; Barabási and Stanley, 1995; Halpin-Healy and Zhang, 1995). In addition to invasion processes in population biology (O'Malley et al., 2006b), roughened fronts emerge commonly in other systems, including the growth of cancerous tumors (Brú et al., 2003), task-completion landscapes in massively parallel computer networks (Korniss et al., 2000, 2003), and surface growth in materials science (Barabási and Stanley, 1995). Models built on quite different assumptions can roughen in the same way; features dependent on roughening will then behave similarly across models.

We recently analyzed the time course of roughening in our two-species model for competitive invasion (O'Malley et al., 2006b). In this paper, we focus on properties of the invader's extreme advance, the front-runner's location (Ellner et al., 1998). We investigate effects of stochasticity, discreteness, and habitat size on the invasion process (Habitat, or landscape, size refers to the linear extent of the system transverse to the direction of invasive advance). For particular parameter values and initial conditions, our model for spatial invasion becomes equivalent to the contact process (CP) (Harris, 1974; Durrett and Levin, 1994a; Hinrichsen, 2000; Oborny et al., 2005). Another parameter set produces a variant of the Eden model (Eden, 1961; Jullien and Botet, 1985a, 1985b; Kawasaki et al., 2006); both CP and the Eden model have served as archetypes for modeling invasive spread. We aim to extract features common to a family of models (hence, characteristics of a universality class). To do so, we first investigate the scaling behavior of our model's interface width (variability of the invader's advance about its mean position), both as a function of time and of habitat size. We then address the shape of the probability density of the front-runner's position. Our analyses reveal consistent universalities. Model details, of course, affect nonuniversal coefficients (or prefactors), but universal features lead to predictions spanning an important class of stochastic growth models. Furthermore, although the front's velocity depends on details of a model's local birth and death rates, the approach to the front's asymptotic velocity—again, as a function of time and of habitat size—is universal, and these dependencies offer a useful tool for identifying ecologically salient properties of a given invasive front.

1.1. Advancing fronts: background comment

Spatial expansion characterizes biological invasion from local to geographic scales (Minogue and Fry, 1983; van den Bosch et al., 1992; Shigesada and Kawasaki, 1997). Selecting a framework for modeling spatially detailed, invasive growth has been posed

as a choice between reaction–diffusion equations for continuous densities or stochastic discrete (individual-based) models (Durrett and Levin, 1994b). The former include deterministic reaction–diffusion systems, which often permit approximation of the invader's speed as the asymptotic velocity of a traveling wave (Dwyer and Elkinton, 1995; Caraco et al., 2002; Murray, 2003). Significant generalizations of the basic deterministic theory vary schedules of reproduction or the distribution of dispersal distance (Cantrell and Cosner, 1991; Shigesada et al., 1995; Kot et al., 1996; Neubert and Caswell, 2000; Dwyer and Morris, 2006) and treat advancing fronts as a traveling waves with constant or increasing velocity. However, traveling waves invoke infinitesimal population densities (van Baalen and Rand, 1998). The front can be “pulled” by growth and spread of the invader at locations where its density is near 0 (Snyder, 2003); the model may consequently overlook realistic features of the dynamics of rarity (Lewis, 2000; Clark et al., 2003; Antonovics et al., 2006). That is, deterministic reaction–diffusion equations are not capable of capturing ecologically relevant effects of spatially correlated variability along the types of fronts we study.

Nevertheless, stochastic partial differential equations (or Langevin equations) and equivalent field-theoretical descriptions have, for decades, been employed successfully as coarse-grained (i.e., “mesoscopic,” continuous-density) representations of both interacting particle systems in physics and chemistry (Korniss and Schmittmann, 1997; Pechenik and Levine, 1999), and individual-based models in biology (Moro, 2001; Escudero et al., 2004). In principle, for every individual-based model one could in the continuous-time limit, construct a dynamically faithful coarse-grained representation using a stochastic partial differential equation (van Kampen, 1981; Gardiner, 1985; Schmittmann and Zia, 1995; Hinrichsen, 2000). Deriving the appropriate noise terms presents a challenge, and the resulting model, with some exceptions, will not likely yield an analytically tractable solution. One then often resorts, as in the case of individual-based models, to numerical investigation. The important point, for questions we address, is that properly developed Langevin equations (van Kampen, 1976; Doi, 1976; Peliti, 1985) and spatially explicit, individual-based models should exhibit identical scaling behavior when critical, large-scale levels of variability govern properties of the invasion dynamics. We therefore choose the more familiar individual-based approach (DeAngelis and Gross, 1992).

Individual-based constructions capture effects of nonlinearity and stochasticity governing invader dynamics at introduction and at an advancing front (Wilson et al., 1993; Wilson, 1998; Thomson and Ellner, 2003). For both individual-based and stochastic partial differential equation models, if diffusion is limited, the front is usually “pushed” at a velocity less than that of the corresponding deterministic diffusion model (Moro, 2003). Furthermore, fronts in these stochastic models roughen; that is, they fluctuate strongly (Kardar et al., 1986). Given an initially flat interface between species, the invader quickly advances different distances along the length of the front. As the front roughens, the size of random fluctuations along the front become spatially correlated (Rácz and Gálfı, 1988; ben-Avraham, 1998; Majumdar and Comtet, 2004), and this correlated variation exerts significant, time-dependent effects on the front's velocity (Krug and Meakin, 1990; van Saarloos, 2003). Roughening also implies that the time-dependent position of the invader's furthest advance, the “front-runner,” will be influenced by the same spatial correlations. One-dimensional models cannot, of course, generate a roughened front.

Our analysis of the front runner's position involves the extreme value among strongly correlated random variables; Fisher and Tippett (1928) and Gumbel (1958) first derived

the distribution of the extreme value among independent random variables. For roughened interfaces, results for independent (or weakly-correlated) random variables break down because of the strongly correlated levels of variability along the front. Recently Majumdar and Comtet (2004, 2005) analytically obtained the scaling behavior of the distribution of the extreme advance of the Kardar–Parisi–Zhang interface (Kardar et al., 1986). The interface-set that emerges in invasion models studied here belongs precisely to this universality class; hence one immediately obtains the shape of the probability distribution of the extreme advance (the front-runner) in the steady state.

2. Model

Invaders often must overcome competition (Elton, 1958; Parker and Reichard, 1998; Hoopes and Hall, 2002; Simberloff et al., 2002) to advance spatially. We assume preemptive competition; neither species can colonize an occupied site until the occupant's mortality opens that site (Comins and Noble, 1985; Connolly and Moko, 2003; Tainaka et al., 2004; Yurkonis and Meiners, 2004). Since we address frontal advance, we ignore introduction from beyond the habitat; a species may occupy new sites only through local propagation when one or more of its nearest-neighboring sites is empty. Although some invasions may be driven by long-distance dispersal (Ferrandino, 1996; Lewis, 1997; Clark et al., 2001), our assumption of limited dispersal has clear empirical justification. D'Antonio (1993) reports that 98% of an invasive succulent's (*Carpobrotus edulis*) population growth over 4 years resulted from spatially clustered clonal propagation. Invasive Argentine ants (*Linepithema humile*) advance spatially by locally budding new from existing colonies (Holway, 1998). For many invasive plants, and some invading animals, phalanx-like advance should prove realistic within any single habitat. Importantly, we note that adding explicit finite-range diffusion, with a small rate, to local colonization does not change the universal aspects of the quantities studied here (Moro, 2001).

2.1. Model dynamics and simulation

On an $L_x \times L_y$ lattice, a site represents the minimal resources necessary to maintain a single individual. The local occupation number at site \mathbf{x} is $n_i(\mathbf{x}) = 0, 1$ with $i = 1, 2$, referring to the resident and invader species, respectively. During a single time unit, one Monte Carlo step per site [MCSS], $L_x L_y$ sites are chosen randomly for updating. An empty site may be occupied by species i through propagation from a neighboring site at rate $\alpha_i \eta_i(\mathbf{x})$, where α_i is the individual-level propagation rate for species i , and $\eta_i(\mathbf{x}) = (1/\delta) \sum_{\mathbf{x}' \in \text{nn}(\mathbf{x})} n_i(\mathbf{x}')$ is the density of species i in the neighborhood around site \mathbf{x} ; $\text{nn}(\mathbf{x})$ is the set of nearest neighbors of site \mathbf{x} , and δ is the number of sites in that neighborhood ($\delta = |\text{nn}(\mathbf{x})|$). Unless noted otherwise, the results presented here are for $\delta = 4$, but in a few cases we set $\delta = 8$ (Moore neighborhood) and $\delta = 12$ (Moore neighborhood plus 4 sites) for comparison. An occupied site opens through mortality of the individual. We assume density-independent mortality (Cain et al., 1995) and assign each species the same mortality rate μ . Summarizing transition rules for an arbitrary site \mathbf{x} , we have

$$0 \xrightarrow{\alpha_1 \eta_1(\mathbf{x})} 1, \quad 0 \xrightarrow{\alpha_2 \eta_2(\mathbf{x})} 2, \quad 1 \xrightarrow{\mu} 0, \quad 2 \xrightarrow{\mu} 0, \quad (1)$$

Table 1 Definitions of model variables and parameters

Symbols	Definitions
$L_x, L_y (= L)$	Lattice size
\mathbf{x}	Location of lattice site
$n_1(\mathbf{x})$	Occupation number for residents at site \mathbf{x} ; $n_1(\mathbf{x}) = 0, 1$
$n_2(\mathbf{x})$	Occupation number for invaders at site \mathbf{x} ; $n_2(\mathbf{x}) = 0, 1$
$\text{nn}(\mathbf{x})$	Set of nearest neighbors around site \mathbf{x}
δ	Size of neighborhood around site \mathbf{x} ($\delta = \text{nn}(\mathbf{x}) $)
$\eta_i(\mathbf{x})$	Density of species i on $\text{nn}(\mathbf{x})$
α_i	Individual rate of propagule production, species i
μ	Mortality rate
$\alpha_c(\mu)$	Minimal propagation rate for persistence
$h_y(t)$	Rightmost invader in row y at time t
$\bar{h}(t)$	Mean of $h_y(t)$
$h_{\max}(t)$	Rightmost invader at time t
$\Delta_{\max}(t) = h_{\max}(t) - \bar{h}(t)$	Distance from front-runner to mean of front
v^*	Asymptotic velocity of invasive front
$\langle w^2 \rangle$	Mean squared interface width
$\xi(t)$	Correlation length along front
α	Roughness exponent
β	Growth exponent
z	Dynamic exponent
ρ_i^*	Equilibrium single-species density
N^*	Number of invaders in a row through the width w

where 0, 1, 2 indicates whether a site is open, resident-occupied, or invader-occupied, respectively. Table 1 defines the symbols and notation we use.

We assume that interspecific competition drives the dynamics (i.e., each species persists absent competition), and that the invader has a reproductive advantage. Therefore, we restrict attention to the $\alpha_c(\mu) < \alpha_1 < \alpha_2$ regime, where $\alpha_c(\mu)$ is the critical propagation rate below which either species, in the other's absence, grows too slowly to avoid extinction (Oborny et al., 2005; O'Malley et al., 2006a).

We impose periodic boundary conditions along the y -direction of the $L_x \times L_y$ lattice. The initial condition is a flat linear front (straight vertical line), i.e., the invader completely occupies a few vertical columns at the left edge of the lattice, and all remaining sites are occupied by the resident. Invasive advance, therefore, proceeds in the x -direction. As a simulation begins, mortality quickly reduces the density on each side of the front to the respective "quasi-equilibrium" value, where a species' propagation balances its mortality. As a simulation continues, we track the location of the invading front by defining the edge as the location of the right-most individual of the invading species, $h_y(t)$, for each row y (Fig. 1). We shall also refer to this quantity as the local "height" [borrowing terminology from the nonequilibrium surface and interface-growth literature (Barabási and Stanley, 1995)]. We record the average position $\bar{h}(t) = (1/L_y) \sum_y h_y(t)$ for each time step. We estimate velocity once $\bar{h}(t)$ approaches linear increase with time. We ran each simulation until the front reached the end of the system. Longitudinal system size L_x has no particular impact on system behavior. But the transverse system size L_y plays a fundamental role in controlling the large-scale properties of the emerging fronts and the interface region. Hence, the size of the habitat (specifically, the length of the front) will exert an important influence on the dynamics of ecological invasion.

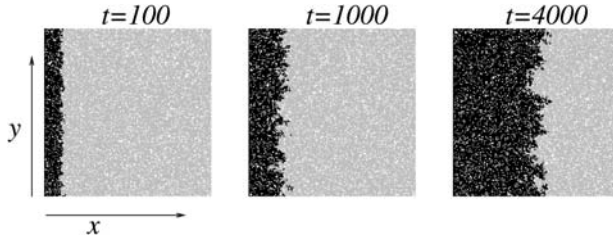


Fig. 1 Snapshots of advancing fronts for transverse system size $L \equiv L_y = 200$ and $\alpha_1 = 0.70$, $\alpha_2 = 0.80$, $\mu = 0.10$. Time has units of Monte Carlo steps per site (MCSS). White cells represent empty sites, while gray and black correspond to sites occupied by residents and invaders, respectively.

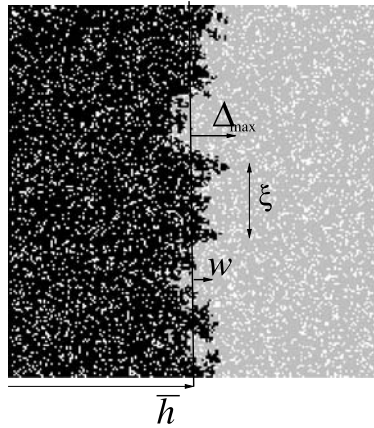


Fig. 2 Width (w) and the extreme advance (Δ_{\max}) relative to the mean front position (\bar{h}) in a rough front. For illustration, correlation length ξ is also indicated.

If the resident is absent initially, model assumptions preclude its introduction. Eliminating the resident species (i.e., $n_1(\mathbf{x}) \equiv 0$ for all \mathbf{x}) reduces the model to the basic contact process for invaders. Furthermore, for the specific choice of $\mu = 0$ (i.e., no mortality), the CP itself reduces to a variant of the Eden model (Jullien and Botet, 1985a). To emphasize the strength of the universal aspects of these stochastic growth processes, we also present some results on the front’s extreme advance for these special parameter choices.

An advancing front “roughens” (Fig. 1). That is, the typical size of deviations about the mean front position increases until the distribution of the mean squared fluctuation equilibrates statistically. The resulting steady-state depends on habitat size L_y (Barabási and Stanley, 1995; Halpin-Healy and Zhang, 1995). Figure 2 shows a typical configuration with “width” w about the front’s average position $\bar{h}(t)$. Similar “wavy” front configurations can be observed in results plotted in recent front-velocity studies of the basic CP (Ellner et al., 1998) and of the Eden model (Kawasaki et al., 2006). This “waviness” is at the heart of kinetic roughening, the focus of our investigation. We emphasize that as habitat size L_y increases, the amplitude of the interface fluctuations (deviations about the mean) in the steady state increases monotonically. In turn, one can employ universality

arguments and recent results to find the shape of the distribution of the front-runner's relative position (Majumdar and Comtet, 2005) and important habitat-size dependent corrections to the velocity of invasive advance (Krug and Meakin, 1990).

3. Roughening of the front

Next, we apply a framework for dynamic scaling of roughened interfaces to advance a new perspective on invasion ecology. To analyze roughening we define the “width” of the invading front via:

$$w^2(L_y, t) = \frac{1}{L_y} \sum_{y=1}^{L_y} [h_y(t) - \bar{h}(t)]^2. \quad (2)$$

Of course, $w^2(L_y, t)$ is itself a fluctuating quantity, so in simulations we estimate an ensemble average over different runs, or take an average over a time series in steady state, to obtain $\langle w^2(L_y, t) \rangle$. Hereafter, we let $L \equiv L_y$, for convenience, and write $\langle w^2(L, t) \rangle$. Without creating confusion, we shall use the notation $w = \sqrt{\langle w^2(L, t) \rangle}$, to refer to the typical size of the interface region.

$w^2(L, t)$ in Eq. (2) is a function of the local stochastic invasion heights $h_y(t)$, and the $h_y(t)$ are not independent random variables. Starting with a flat interface, a single correlation length $\xi(t)$ develops along the front (Fig. 2). This correlation length grows as a power-law function of time $\xi(t) \sim t^{1/z}$ (Barabási and Stanley, 1995), but once $\xi(t)$ spans the length L of the system, at a crossover time on the order of $t_x \sim L^z$, roughening has reached its stationary state. The heights of invasive advance along the front have become and remain dependent random variables, complicating analysis of the invader's maximal advance (Raychaudhuri et al., 2001; Majumdar and Comtet, 2004). We let $\langle w^2(L, \infty) \rangle$ represent the mean squared deviation when its distribution has equilibrated; below we focus our front-runner analysis on these steady-state fluctuations.

Advancing fronts with different locally structured propagation and mortality processes may still exhibit the same dependence of roughening on time, and the equilibrium variability along the front may exhibit the same dependence on habitat size. Such fronts belong to the same “universality class”; universality offers powerful simplification and generalization (Cardy, 1996; Ferreira and Alves, 2006). O'Malley et al. (2006b) found that our model's roughening behavior belongs to the KPZ universality class (for Kardar–Parisi–Zhang; see Kardar et al., 1986). We summarize those results, since quantifying roughening allows us to correct the asymptotic velocity of invasion, and to write the probability density of the front runner's relative position. Appendix B provides some further details about the KPZ equation, a continuous stochastic differential equation that captures interface dynamics for a large class of discrete, stochastic individual-based systems.

The profound nature of roughened fronts (or self-affine interfaces) lies in the intimate connection between their temporal and spatial scaling behavior (Barabási and Stanley, 1995; Halpin-Healy and Zhang, 1995). For a system with transverse system size L , for early times, the width (or spread) of the interface [Figs. 1, 2] increases in a power-law fashion $\langle w^2(L, t) \rangle \sim t^{2\beta}$. Then after a system-size dependent cross-over time $t_x \sim L^z$, the front reaches its steady-state: interface fluctuations about the steadily advancing mean

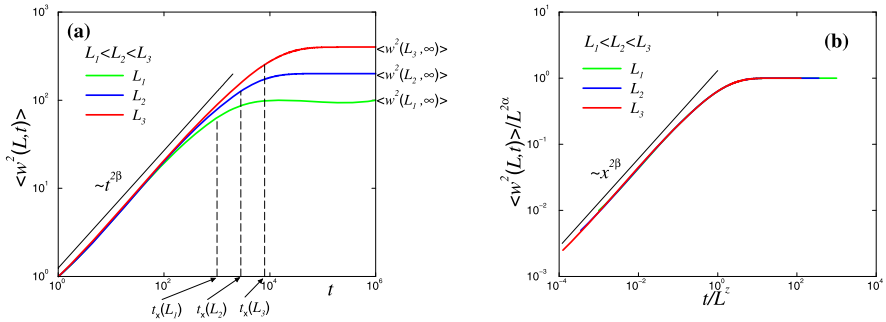


Fig. 3 Schematic plot illustrating the scaling features of the width of rough fronts, Eq. (3). (a) Interface width vs. time on log-log scales, for different system sizes $L_1 < L_2 < L_3$. For early times, the width of the interface increases as $\langle w^2(L, t) \rangle \sim t^{2\beta}$. After a system-size dependent cross-over time $t_x(L) \sim L^z$, the interface fluctuations become stationary, and the width reaches its system-size dependent steady-state value $\langle w^2(L, \infty) \rangle \sim L^{2\alpha}$. The straight solid line corresponds to the power-law increase for early times before the crossover (growth phase). For larger transverse system size L , it takes longer to reach steady state, and the width in the steady state is larger. (b) Scaled plot $\langle w^2(L, t) \rangle / L^{2\alpha}$ vs. t/L^z , yielding full data collapse for different system sizes, the signature of dynamic scaling (Barabási and Stanley, 1995). The straight solid line indicates the power-law behavior $x^{2\beta}$ of the scaled variable $x = t/L^z$ for $x \ll 1$.

front become stationary, but their magnitude will depend on the transverse system size. In particular, the interface width “saturates” in time, and its stationary value will scale with the system size as $\langle w^2(L, \infty) \rangle \sim L^{2\alpha}$. Thus, both the time to reach steady state and the size of the steady-state width depend on the transverse system size L in a power-law fashion. Put simply, if the transverse system size is increased, both the time to reach steady state and the width of the interfacial region in the steady state increase. The exponents $\alpha > 0$, $\beta > 0$, and $z > 0$ are referred to as the roughness, growth, and dynamic exponent, respectively. (The roughness exponent α should not to be confused with the local propagation rates of the two species.) These fundamental scaling properties of roughening can be summarized as

$$\langle w^2(L, t) \rangle \sim \begin{cases} t^{2\beta} & \text{for } t \ll t_x, \\ L^{2\alpha} & \text{for } t \gg t_x, \end{cases} \quad t_x \sim L^z \tag{3}$$

and are illustrated schematically in Fig. 3. In general, these exponents obey a scaling relationship $\alpha = \beta z$ (Barabási and Stanley, 1995).

Models whose kinetic roughening can be described by the same set of exponents are said to belong to the same *universality class* (Barabási and Stanley, 1995; Halpin-Healy and Zhang, 1995). Fronts generated by models with different local rules often belong to the same universality class (for example, fronts in the Eden model, the contact process, and the two-species model of this paper). Importantly, models formulated to address completely different questions, ranging from surface physics and computer science (Korniss et al., 2003) to ecology, can belong to the same universality class.

The front in our two-species individual-based model exhibits scaling consistent with Expression (3); the exponents are $\beta = 1/3$, $\alpha = 1/2$, and $z = 3/2$ (O’Malley et al., 2006b). Consequently, the front belongs to the so called KPZ-interface universality class

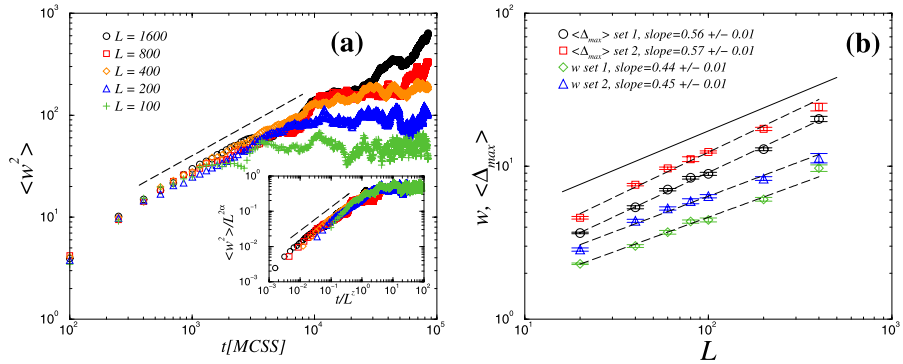


Fig. 4 (a) Average width as a function of time (log-log scales) for various system sizes, averaged over 20 independent realizations with $\alpha_1 = 0.70$, $\alpha_2 = 0.80$, and $\mu = 0.10$. Dashed line corresponds to the one-dimensional KPZ power law with the exponent $2\beta = 2/3$. Inset shows the scaled plot, $\langle w^2(L, t) \rangle / L^{2\alpha}$ vs. t/L^2 using the KPZ exponents. (b) Steady-state width, $w = \sqrt{\langle w^2(L) \rangle}$, and extreme fluctuations, $\langle \Delta_{\max}(L) \rangle$, (averaged over time series in the steady-state) as a function of system size, L ($\equiv L_y$), for two sets of parameters: Set 1 ($\alpha_1 = 0.50$, $\alpha_2 = 0.70$, and $\mu = 0.20$); and Set 2 ($\alpha_1 = 0.70$, $\alpha_2 = 0.80$, and $\mu = 0.10$). Dashed lines indicate the best-fit power laws. The solid line corresponds to the theoretical asymptotic scaling in the KPZ universality class with roughness exponent $\alpha = 1/2$.

(in one transverse dimension) (Fig. 4). Slight deviations from the theoretical exponents result, in part, from corrections to scaling and “intrinsic width” effects for limited system sizes (Moro, 2001; Blythe and Evans, 2001). Furthermore, the strong correlation in the steady-state time series of $w^2(t)$ (the auto-correlation time also diverges with the system size as L^2) increases sampling error for larger system sizes. For the KPZ universality class, the analytical result by Foltin et al. (1994) specifies the universal shape of the distribution of the steady-state width (see Appendix B.2). The results can be used to identify the universality class of a model with a rough front; doing so provides further support that our model belongs to the KPZ class (Appendix B.2).

3.1. Roughening and the asymptotic invasion velocity

Estimating the speed at which an invasive species advances remains a focus of ecological theory (Mollison and Levin, 1995; Ellner et al., 1998; Lewis, 2000; Kawasaki et al., 2006). Finding an analytical expression for a stochastic front’s asymptotic velocity v^* presents a challenge (Pechenik and Levine, 1999), particularly for two-dimensional fronts. Analytically tractable, pulled fronts emerge naturally in the deterministic reaction–diffusion limit of our model (Fisher, 1937; Holmes et al., 1994; Dwyer and Elkinton, 1995; Murray, 2003; van Saarloos, 2003) (see Appendix A). But their velocity typically overestimates that of the actual individual-based model in the diffusion-limited regime (Moro, 2001, 2003; Doering et al., 2003). Our model, with only local dispersal and no “explicit” diffusion, lies precisely in that regime: since interspecific mixing is insufficient about the interface, and internal fluctuations are important, deterministic equations break down (Antonovics et al., 2006; O’Malley et al., 2006b).

Deterministic reaction–diffusion models neglect discreteness of individuals, the fundamental source of endogenous fluctuations (Escudero et al., 2004). Consequently, de-

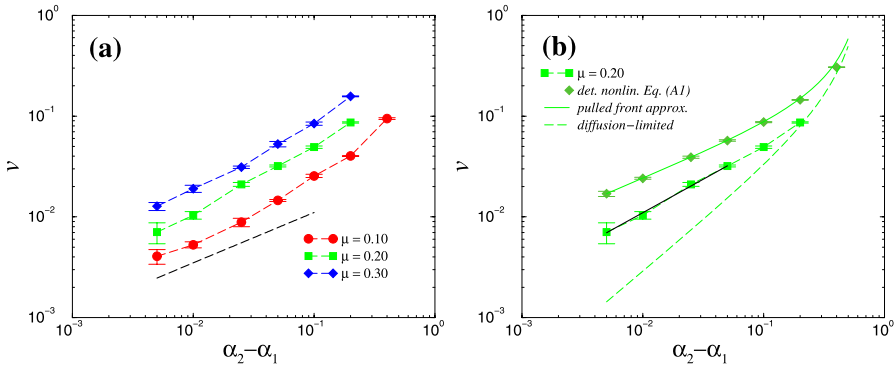


Fig. 5 (a) Asymptotic front velocities from Monte Carlo simulations of the individual-based stochastic model for fixed $\alpha_2 = 0.70$, as a function of the difference between propagation rates, $\alpha_2 - \alpha_1$, with $L_y = 100$, for three values of μ . (b) Simulation results from (a) for $\mu = 0.20$ compared with the results from numerically iterating the deterministic nonlinear reaction–diffusion equations, Appendix A, Eq. (A.1) (O’Malley et al., 2006b, 2009) and with two approximate analytic limits: pulled-front approximation [solid curve, Eq. (A.4)] and diffusion-limited front (dashed curve, Moro, 2003). The solid straight line is the best-fit effective power law in the region where the difference between propagation rates is small, corresponding to $v \sim (\alpha_2 - \alpha_1)^\theta$ with $\theta = 0.66 \pm 0.04$.

terministic reaction–diffusion theory neglects the substantial, correlated random variation in the extent of the invader’s advance along the front. To demonstrate the significance of this difference, we compared results from Monte Carlo simulation of the individual-based model defined by the transition rates in Eq. (1) to the velocity of traveling waves (pulled fronts) arising in our model’s deterministic reaction–diffusion limit, $v_p = (\mu/\alpha_1)\sqrt{\alpha_2(\alpha_2 - \alpha_1)}$ (see Appendix A). Asymptotic invasion velocity v_p increases as either the common mortality rate μ or competitive asymmetry, $(\alpha_2 - \alpha_1)$, increases; a strong resident competitor can slow an invasive species’ advance under a variety of assumed dynamics (Hosono, 1998; Gandhi et al., 1999; Weinberger et al., 2002; O’Malley et al., 2009). For further comparison with our stochastic model, note that the traveling wave approaches its steady-state value as $v(t) = v_p - \mathcal{O}(1/t)$; that is, the traveling wave’s temporal correction decays as t^{-1} (Holmes et al., 1994).

Figure 5(a) plots asymptotic velocities from simulation of our individual-based model (for fixed α_2) as a function of competitive asymmetry $(\alpha_2 - \alpha_1)$. For parameter values chosen, the invader advances more slowly than our model’s deterministic reaction–diffusion limit (i.e., slower than v_p) [Fig. 5(b)]. It is important to note that the pulled front approximation v_p can fully reproduce the numerical solutions of the *deterministic nonlinear* reaction–diffusion system [Appendix A, Eqs. (A.1) and (A.2)] (O’Malley et al., 2006b, 2009). What it fails to account for are the effects of *stochasticity*. In our discrete, stochastic model the front becomes pushed (van Saarloos, 2003); invasion velocity depends on the full frontal region, with its nonlinear interactions, rather than depending on the leading edge only (a pulled front). For comparison, we also plot an approximate expression for the velocity, suggested by Moro (2003), $v_{DL} = \mu(\alpha_2/\alpha_1 - 1)$, applicable to strongly diffusion-limited systems (see next section), where the effective diffusion coefficient is negligible compared to the effective reaction rates. As Fig. 5(b) shows, except for large $(\alpha_2 - \alpha_1)$, this approximation underestimates the front velocity of our individual-based model. This

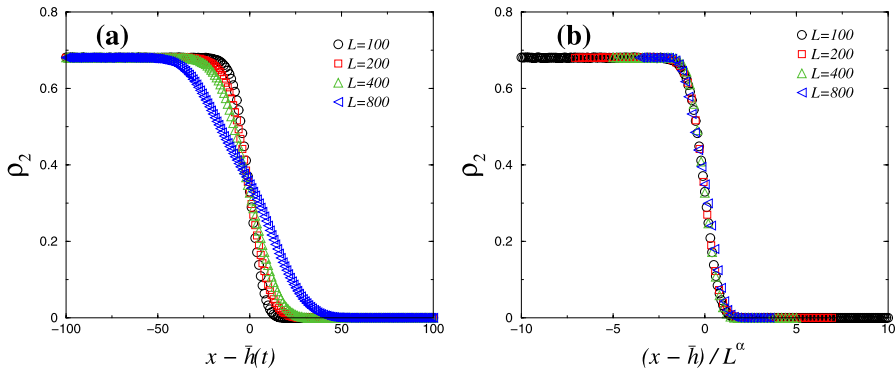


Fig. 6 (a) Steady-state spatial density profiles of the invader species [averaged over all rows, Eq. (4)] for several habitat sizes, for parameter “Set 1” ($\alpha_1 = 0.50$, $\alpha_2 = 0.70$, $\mu = 0.20$), averaged over 10^4 time steps. (b) Same data as in (a), but scaled according to the system-size dependent width of the front ($w \sim L^\alpha$ with $\alpha = 1/2$).

may be expected by noting that the effective reaction and diffusion coefficients are of the same order of magnitude (see Appendix A).

The functional expression for a model’s asymptotic velocity cannot be universal, since it must depend on details of the local dynamics. However, Krug and Meakin (1990) showed that temporal and finite-size ($L_y = L$) corrections to the asymptotic velocity are universal within a given class (see Appendix B.3); a general ecological prediction consequently emerges. Frontal velocity initially increases until reaching steady state. Prior to the steady state, the difference between the current and asymptotic velocities (the temporal correction) scales similarly with time for every member of a particular universality class. More importantly, the second correction recognizes that steady-state velocity depends on habitat size; the habitat-size correction is proportional to L^{-1} [see Appendix B.3, Eq. (B.6)]. That is, a given invasive species’ front will advance faster as linear habitat size increases. More generally, the finite-size correction to the asymptotic velocity scales similarly with habitat size for each stochastic model where invasive advance exhibits a KPZ interface.

3.2. Invader spatial profiles and diffusion limitation

Next, we focus on invader density within the width of the advancing front, to compare stochastic and deterministic invasion models in a general context. We constructed density profiles for the invader along the horizontal direction (averaged over rows y , for a given x):

$$\rho_2(x) = \frac{1}{L_y} \sum_{y=1}^{L_y} n_2(x, y). \quad (4)$$

The density profile should spread horizontally in response to the front’s roughening (as a function of time during growth phase, and as a function of habitat size in steady state). Figure 6(a) shows the invader’s steady-state density profiles as a function of distance

from the front's mean position. Profiles are averaged over 10^4 time steps, and plotted for a series of habitat sizes L . Behind the front, where the resident has been excluded, invader density $\rho_2(x)$ rests at its single-species equilibrium ρ_2^* . Invader density declines through the width, and only the resident occupies locations well right of the front.

The steady-state density profiles show that the span of the frontal region, within which $\rho_2^* > \rho_2(x) > 0$, increases progressively with habitat size L [Fig. 6(a)]. Since steady-state roughening scales with habitat size according to $\langle w^2(L, \alpha) \rangle \sim L^{2\alpha}$, rescaling the abscissa by L^α ($= L^{1/2}$) results in the different density profiles falling on the same plot [Fig. 6(b)], an articulate data collapse indicating the fundamental, underlying dependence (cf. Antonovics et al., 2006).

We stress that expansion of density profiles with increasing habitat size is not a result of greater mixing of the two species within the span of the front. Rather, density profiles result from emerging spatial correlations between fluctuations in the invader's advance along the length of the front, a collective result of the neighborhood-level stochastic dynamics. Indeed, spatial configurations in Figs. 1 and 2 reveal that few single rows, if any, suggest an invader-density gradient. In fact, the density profile in most rows resembles a "shock-wave."

Moro (2003) analyzes transitions from pushed-front to pulled-front velocities in discrete, stochastic models. Our simulations fall into Moro's diffusion-limited regime, where strong spatial correlations produced by local propagation dominate effects of mixing along the front. Our model's assumptions (in particular, no explicit diffusion) and parameter values imply that the mean-field assumption of strong mixing at the between-species interface cannot hold. Consequently, our competitive invasion produces, in any given row, an invader-density gradient that spans only a narrow region; essentially, the invading species advances as a shockwave front. Moro's (2003) analysis identifies the significance of N^* , the (approximate) number of invaders occupying a row of the interface between the two regions of single-species equilibrium densities. The front's velocity asymptotically approaches the reaction-diffusion (pulled-front) velocity v_p only as $N^* \rightarrow \infty$. For a mortality rate of $\mu = 0.1$, our simulations have $1 < N^* < 2$, so that the impact of discreteness and stochasticity remains strong.

4. The front-runner: roughening and scaling of extremes

Finally, we turn to the problem of the invading species' "front-runner" (Ellner et al., 1998; Clark et al., 2001; Thomson and Ellner, 2003), and scaling of the distribution of the maximal invasive incursion. The front-runner's position presents an extreme value problem, complicated by the probabilistic, strongly correlated dependence of the invader's advance at different locations along the front (Raychaudhuri et al., 2001; Majumdar and Comtet, 2004). Hence, traditional extreme-value statistics (Fisher and Tippett, 1928; Gumbel, 1958; Berman, 1964; Galambos, 1987; Galambos et al., 1994) are not applicable.

We restrict attention to height fluctuations occurring after roughening has equilibrated ($t \gg t_x \sim L^z$). At each time step, we identify the farthest-advanced location of the invading species, $h_{\max}(t) = \max_y \{h_y(t)\}$. Measuring the extreme advance relative to the front's mean position, $\bar{h}(L, t)$, we obtain the maximal relative height at time t , $\Delta_{\max}(t) = h_{\max}(t) - \bar{h}(L, t)$. We sample $\Delta_{\max}(t)$ sufficiently to construct histograms

to estimate the probability density of the extreme fluctuations $P(\Delta_{\max}, L)$, for different propagation/mortality rates, and for different habitat sizes L .

Results presented above led us to conclude that the front in our two-species invasion model belongs to the KPZ class. Hence, we can proceed to characterize properties of invasive extremes. Given steady-state roughening of the invading species' front, the probability density of the extremes can be written as

$$P(\Delta_{\max}, L) = \frac{1}{\langle \Delta_{\max} \rangle} \Psi(\Delta_{\max}/\langle \Delta_{\max} \rangle), \quad (5)$$

where $\Psi(u)$ is the probability density of the scaled variable $u = \Delta_{\max}/\langle \Delta_{\max} \rangle$ and is independent of habitat-size L . $\Psi(u)$ is a scaled Airy density for all interfaces belonging to the KPZ universality class (Majumdar and Comtet, 2004, 2005) (see Appendix B.4). Importantly, the steady-state average of the extreme advance scales with the habitat size in the same fashion as the width w , i.e., $\langle \Delta_{\max} \rangle \sim L^\alpha$ with $\alpha \approx 1/2$ [Fig. 4(b)]. That is, the expected displacement of the front-runner ahead of the invader's mean position increases with habitat size in the above power-law fashion. Again, certain system-specific characteristics still depend on local rates, neighborhood size, etc., but our general ecological prediction does not depend on these details.

Figure 7(a, b) provides an example, using two different sets of parameters. As habitat size increases, the mode and dispersion of the estimated probability densities $P(\Delta_{\max}, L)$ increase, driven by the dependence of $\langle \Delta_{\max} \rangle$ on L . Rescaling these positively skewed histograms, and plotting the resulting distributions of $(\Delta_{\max}/\langle \Delta_{\max} \rangle)$, collapses the data articulately for all system sizes and both sets of parameters onto the (theoretical) scaled Airy density [Fig. 7(c, d)]. Note that no fits are used in collapsing the scaled data with the theoretical curve. The largest deviations from the theoretical prediction can be observed around the peak of the distributions for some larger system sizes. This poorer statistical sampling is, in part, due to the correlated nature of the steady-state time series of the extremes, which is progressively more significant for larger system sizes.

Longer fronts increase the expected maximal difference between locations of the front runner and the front's mean position. The scaling of the front runner's relative position is possible because the distribution of the extremes is governed by this single scaling $\langle \Delta_{\max} \rangle \sim L^{1/2}$. Note that traditional extreme-value limit theorems (Gumbel, 1958; Fisher and Tippett, 1928; Berman, 1964) for weakly or uncorrelated fluctuations along the front would yield only a weak logarithmic increase with the habitat size L (Raychaudhuri et al., 2001; Guclu and Korniss, 2004).

To emphasize the significance of universality, we repeated some of our analyses for the extremes of the front and compared our model's behavior with two other, well known invasion models, the Eden model and the basic contact process. We note that the fronts in both of these models have long been believed to belong to the KPZ class (Jullien and Botet, 1985a, 1985b; Plischke and Rácz, 1985; Kertész and Wolf, 1988; Moro, 2001; Ferreira and Alves, 2006). The scaled probability densities exhibit the expected, progressive data collapse on to the universal Airy distribution [Fig. 8]. The scaled extreme-distribution plots include not only different models and system sizes, but for illustration, different neighborhood sizes as well ($\delta = 4, 8, 12$ for the contact process). The Eden model, the basic contact process, and our model of invasion under preemptive competition share scaling properties, revealing common, key properties of their advancing fronts, in

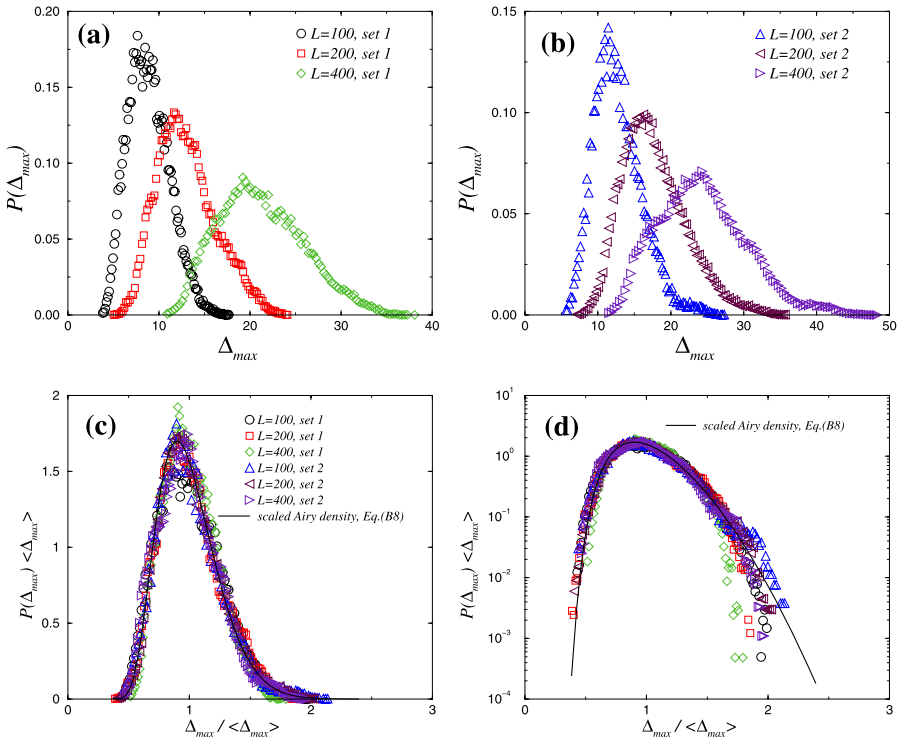


Fig. 7 (a) Steady-state distributions of the extreme advance, relative to mean front, for several habitat sizes. Parameters are $\alpha_1 = 0.5$, $\alpha_2 = 0.7$, and $\mu = 0.2$ (“Set 1”), and (b) for $\alpha_1 = 0.7$, $\alpha_2 = 0.8$, and $\mu = 0.1$ (“Set 2”). (c) Scaled histograms for all habitat sizes, and for both Set 1 and Set 2. The solid curve is the scaled Airy density, Eq. (B.8) (Majumdar and Comtet, 2004). (d) Same data as in (c) but on lin-log scales.

the light of KPZ universality. Consequently, we can infer a series of ecological predictions shared by the most often cited discrete, stochastic models of invasive growth.

5. Discussion

We recently applied theory for nucleation in homogeneous environments to the spatial dynamics of invasion (Korniss and Caraco, 2005; O’Malley et al., 2005, 2006a). Immigration introduces individuals of an initially rare, but competitively superior, invader randomly independently in space and time. An introduced invader, stochastically, may die or may propagate locally and initiate a cluster of invaders. A nucleation event occurs when an invader cluster reaches a critical size where further growth through propagation and decline through mortality have equal probability (Gandhi et al., 1999; Yasi et al., 2006; Allstadt et al., 2007). Supercritical clusters, on average, exhibit radial symmetry and expand at a constant velocity after sufficiently long periods; their growth excludes the resident competitively. Circular fronts will reach the same final velocity as their linear coun-

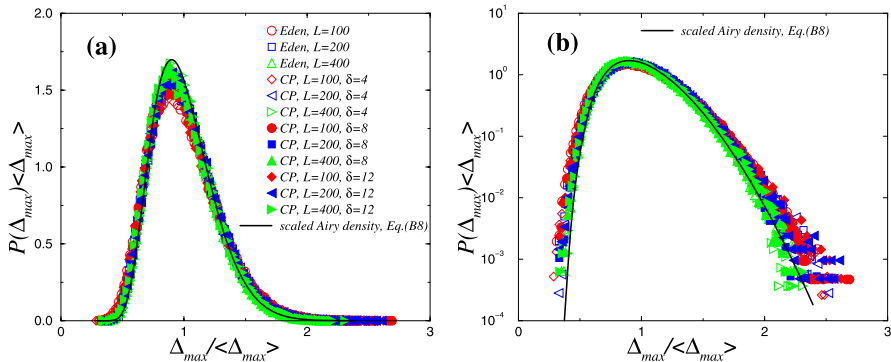


Fig. 8 (a) Scaled steady-state distributions of the extreme advance for the contact process (CP) and for the Eden model for $L = 100, 200, 400$. For both models, there is only one species present (invaders) with local propagation rate α_2 and mortality rate μ . For the CP, we set $\alpha_2 = 1$ and $\mu = 0.20$. The front dynamics of the CP for $\alpha_2 = 1$ and $\mu = 0$ is equivalent to a variant of the Eden model (Jullien and Botet, 1985a, 1985b), and we used these parameter values to obtain the Eden data. For the Eden model, we used only nearest-neighbor propagation ($\delta = 4$). For the CP, we also explored different neighborhood sizes, $\delta = 4, 8, 12$; all are shown on the plot. The solid curve is the scaled Airy density, Eq. (B.8) (Majumdar and Comtet, 2004). (b) Same data as in (a) but on lin-log scales.

terparts, with the same corrections as times increases (O'Malley et al., 2009), so that our analysis of linear fronts furthers application of nucleation theory to the evolutionary ecology of invasion.

To characterize important consequences of discreteness and stochasticity for invasive advance, we introduced kinetic roughening of the invader-resident interface. Roughening of our simulated fronts behaves as a member of the KPZ-universality class in one (transverse) dimension. Since steady-state roughening depends on habitat size, the distribution of the invader's maximal incursion, relative to the front's mean position, also depends on habitat size. The advancing front's steady-state velocity correction varies inversely with habitat size, again a consequence of the two-dimensional stochastic front's roughening.

Kawasaki et al. (2006) report two-dimensional stochastic simulations of an invader advancing into empty space; propagation into an open site can occur if any of its 8 nearest neighbors is occupied. They also assume that invaders are immortal. These assumptions, with growth initiated from a compact region occupied by the invaders, render their model essentially a variant of the Eden model (Jullien and Botet, 1985a). Hence their model should exhibit KPZ roughening (Jullien and Botet, 1985b; Plischke and Rácz, 1985; Kertész and Wolf, 1988; Ferreira and Alves, 2006).

Kawasaki et al. (2006) suggest that stochasticity accelerates invasive advance in their two-dimensional simulations, and that reports of deceleration due to stochasticity may arise because the latter address only one-dimensional processes (Snyder, 2003). Above, we detailed simulation results finding that stochasticity (combined with discreteness) significantly slows the velocity of an invading competitor in two-dimensions. Kawasaki et al.'s (2006) seemingly atypical result reflects the particular deterministic model they compared to their simulations, rather than dimensionality. We compared our stochastic invasion velocities to results from the corresponding reaction-diffusion model, the common baseline approach to invasion velocity in ecology (Andow et al., 1990;

Holmes et al., 1994). In the context of Moro's (2003) analysis, our stochastic model has $1 < N^* < 10$; i.e., less than 10 individuals in each row of the interface width. Our deterministic comparison, the reaction–diffusion model, has $N^* \rightarrow \infty$. Our stochastic velocity is slower due to diffusion limitation; our pushed fronts are slower than a pulled front. Kawasaki et al. (2006) base their claim on comparing stochastic simulations to simultaneous advance of the invader in each row. The invader advances (periodically) as an exactly straight “cliff”; no roughening can occur. Their deterministic comparison behaves as if $N^* \rightarrow 0$, since the front has no width; that is, Kawasaki et al. (2006) compare their stochastic simulations to an idealized pushed front, rather than to a pulled front (both being inadequate to estimate the velocity of strongly-correlated rough fronts).

Antonovics et al. (2006) present a “patch model” where local demes of a single species are coupled by movement between neighboring locations. A gradient in density-independent mortality restricts the species' range, and the density profile predicted by a mean field model reflects the spatial pattern in mortality. Stochastic simulations with small deme sizes produce average density profiles falling below the mean field prediction; increased rates of diffusion diminish effects of stochasticity, and density profiles approach the mean field result (Antonovics et al., 2006). Hence, a reduction in diffusion limitation may accelerate an advancing front or extend a static range boundary.

Our model assumes local propagation only, to simulate limited dispersal. Density profiles at the advancing front strongly constrain mixing of the invader and resident along the interface. The resulting diffusion limitation (Moro, 2001) distinguishes reaction–diffusion velocity from invasion velocities driven strictly by local births, budding, or vegetative propagation. The very narrow region with a nonzero density gradient in any row (along the direction of the invader's advance) of our model's interface indicates little mixing of the two species, and compares well with Holway's (1998) study of the invasive Argentine ant. New colonies lie close to existing colonies. Budding of the invader colonies pushes native ants back as the front advances, and the width of the front between invader and residents apparently remains quite narrow.

Although our model has no explicit diffusion, the coarse-graining procedure does generate, albeit nonlinear, diffusion in the continuum limit (see Appendix A). Including further local diffusive moves in our model will not change its universality class, provided that the effective diffusion coefficient is not much larger than the effective reaction rate (Moro, 2001). Thus, one way to change the asymptotic scaling and the corresponding universality class of the front is to introduce local diffusion with large rates (compared to local propagation), or alternatively, introduce long-range dispersal. In these cases, one expects a crossover from the KPZ class to that of the deterministic reaction–diffusion equation, or similar model (Kot et al., 1996), which exhibits a pulled front.

The dynamical crossover from pushed to pulled fronts may help organize results on the modeling and measurement of invasive growth. Generally, we can associate different fronts with ecological-invasion studies categorized according to the particular spatial scale emphasized. At the within-habitat scale, some plant and animal invaders' spatial growth is driven by neighborhood-level propagation (D'Antonio, 1993; Silvertown et al., 1994; Schwinning and Parsons, 1996; Holway, 1998). The limitation on empirically observed dispersal distances appears consistent with effective-diffusion limitation and pushed fronts, within any habitat invaded successfully. Jump dispersal, at the between-habitat scale, for these same species then must depend on other ecological or cultural processes generating introduction events (Korniss and Caraco, 2005).

As estimated dispersal distances of individuals increase (Andow et al., 1990; Bjornstad et al., 2002), diffusion limitation relaxes, and a reaction–diffusion dynamics may approximate spatial advance reasonably well, at both the within-habitat (Dwyer, 1992; Frantzen and van den Bosch, 2000) and between-habitat (van den Bosch et al., 1992; Nash et al., 1995) scales. Deterministic reaction–diffusion models, as noted above, predict pulled fronts advancing at a constant asymptotic velocity. Another set of invasion models can admit increasing velocities; they emphasize the between-habitat spatial scale and note the importance of long-distance dispersal for some biological invasions (Kot et al., 1996; Cannas et al., 2006). Particular applications include the biogeographical range expansion of tree species, as indicated by paleoecological records (Clark et al., 1998), aerial spread of pathogens at the continental scale (Aylor, 2003), and dispersal vectored by human migratory (Fisher et al., 2001) or economic (Ruiz et al., 2000) activity. Long-distance dispersal events, even if rare, can establish colonies detached from the main body of invaders; the two populations may then grow and coalesce (Shigesada et al., 1995). Invasion dynamics averaging over dispersal-distance distributions associated with these models can predict pulled fronts with an ever-increasing spatial velocity; Clark et al. (2001) discuss details and theoretical modifications.

5.1. *The front-runner*

Our front-runner analyses integrate a series of stochastic spatial models through a few universal scaling relationships. For all models belonging to the KPZ universality class (in one transverse dimension) and for large enough habitat size L , $\langle \Delta_{\max} \rangle \sim L^{1/2}$ [Fig. 4(b)]; the distribution of the scaled probability density is given by the Airy distribution [Figs. 7 and 8]. These universal features will be exhibited by any invasion model belonging to the KPZ class (Plischke and Rácz, 1985; Ferreira and Alves, 2006), not just our two-species model, the contact process, and the Eden model.

We referred to transverse system size $L_y = L$ as habitat size, not ordinarily a “tunable parameter” for probing roughness characteristics of the interface. Furthermore, for simplicity, we employed periodic boundary conditions in the transverse direction. From the viewpoint of empirical application, we can envision a scenario where one has access to only a limited observation window on the full landscape. Designate the window’s size L_{obs} , where $1 \ll L_{\text{obs}} \ll L$. These length scales are measured in units of the minimum linear size needed to sustain a single individual (linear size of a lattice site in simulations). One of the research challenges in extreme-value statistics is to predict some characteristic of the extremes on global scales (i.e., at the entire habitat or landscape level) based on some limited local measurements (i.e., taken from the observation window). One can divide the observation region into a number of smaller nonoverlapping subwindows of size l , such that $1 \ll l \ll L_{\text{obs}}$, and by changing the size of the subwindow l , perform a finite-size analysis to extract estimates for the roughness exponent from the average width and the extremes as $w(l) \sim l^\alpha$ and $\langle \Delta_{\max}(l) \rangle \sim l^\alpha$. The subwindows will now have “window” or free boundary conditions (Antal et al., 2001, 2002; Majumdar and Comtet, 2005), clearly differing from the periodic boundaries we simulated. However, boundary conditions do not affect the roughness exponent, hence the scaling properties of width and that of the extremes with l . Therefore, one can estimate the size of the extremes for the full landscape of size L from measurements obtained in a limited observation window, $\langle \Delta_{\max}(L) \rangle \approx \langle \Delta_{\max}(L_{\text{obs}}) \rangle (L/L_{\text{obs}})^\alpha$. In contrast, were

the interfacial fluctuations weakly- or un-correlated, traditional extreme-value statistics (for short-tailed parent distributions) would apply. In turn, extrapolating local measurements to global scales for the extremes would yield only marginal (logarithmic) increase, $\langle \Delta_{\max}(L) \rangle \approx \langle \Delta_{\max}(L_{\text{obs}}) \rangle [\ln(L)/\ln(L_{\text{obs}})]^{1/\gamma}$, where γ is a nonuniversal exponent, and is related the precise shape of the exponential-like tail of the parent densities (Raychaudhuri et al., 2001; Guclu and Korniss, 2004).

The velocity of spatial advance and the properties of the interface region remain objects of study in population biology because of their conceptual significance and potential importance to applied ecology. Despite attention directed to invasive spatial growth, ecological theory has overlooked the impact of correlations along an advancing front (roughening in a two-dimensional environment). Although these spatial correlations arise through local interactions, at a scale sometimes considered “noise,” they can directly affect population/community-level phenomena: invader velocity, dynamics at the interface, and relative position of the front-runner.

Acknowledgements

We thank B. Kozma for discussions, earlier collaborations (O'Malley et al., 2006b, 2009), and permission to use his data in this work. We are also grateful to S. Majumdar for providing us the numerically evaluated Airy distribution (Majumdar and Comtet, 2004, 2005) shown in Figs. 7 and 8. E. Moro kindly commented on earlier results, and we also appreciate discussion with A. Allstadt and Z. Rácz. We also thank the reviewer for offering useful suggestions. This work was supported in part by the National Science Foundation under Grant Nos. DEB-0324689 and DMR-0426488.

Appendix A: Deterministic reaction–diffusion limit and pulled fronts

O'Malley et al. (2006b) write the master equation corresponding to transition rates in Expression (1) (van Kampen, 1981). Assuming that densities at different sites remain uncorrelated (McKane and Newman, 2004; Korniss and Schmittmann, 1997), one obtains the dynamics of the ensemble-averaged local densities $\rho_i(\mathbf{x}, t) \equiv \langle n_i(\mathbf{x}, t) \rangle$,

$$\begin{aligned} \rho_i(\mathbf{x}, t+1) - \rho_i(\mathbf{x}, t) &= [1 - \rho_1(\mathbf{x}, t) - \rho_2(\mathbf{x}, t)] \\ &\quad \times \frac{\alpha_i}{4} \sum_{\mathbf{x}' \in \text{nn}(\mathbf{x})} \rho_i(\mathbf{x}', t) - \mu \rho_i(\mathbf{x}, t), \end{aligned} \quad (\text{A.1})$$

where $i = 1, 2$ for resident and invader species, respectively, and we let $\delta = 4$ for simplicity. Taking the naive continuum limit of the above equations yields the (coarse-grained) equations of motion

$$\begin{aligned} \frac{\partial \rho_i(\mathbf{x}, t)}{\partial t} &= \frac{\alpha_i}{4} [1 - \rho_1(\mathbf{x}, t) - \rho_2(\mathbf{x}, t)] \nabla^2 \rho_i(\mathbf{x}, t) \\ &\quad + \alpha_i [1 - \rho_1(\mathbf{x}, t) - \rho_2(\mathbf{x}, t)] \rho_i(\mathbf{x}, t) \\ &\quad - \mu \rho_i(\mathbf{x}, t), \end{aligned} \quad (\text{A.2})$$

$i = 1, 2$, and ∇^2 is the Laplacian operator. In statistical physics, equations of this kind are referred to as “mean-field” theory, in the sense that correlations between spatial degrees of freedom are neglected (McKane and Newman, 2004; Antonovics et al., 2006). This contrasts to population biology’s terminology where “mean-field” ordinarily refers to non-spatial models. After adding appropriate noise terms to the above equations, the resulting Langevin equation can, in principle, effectively capture both spatial and stochastic effects, identical to those in the underlying discrete individual-based model (Schmittmann and Zia, 1995; Hinrichsen, 2000; van Kampen, 1981; Gardiner, 1985).

The spatially homogeneous solutions of the above equations, (ρ_1^*, ρ_2^*) , are $(0, 0)$, $(1 - \mu/\alpha_1, 0)$, and $(0, 1 - \mu/\alpha_2)$; coexistence is not feasible. In the parameter regime of interest, $\mu < \alpha_1 < \alpha_2$, only the last solution $(0, 1 - \mu/\alpha_2)$ is stable. The advance of a front separating the stable $(0, 1 - \mu/\alpha_2)$ (invader dominated) and unstable $(1 - \mu/\alpha_1, 0)$ (resident dominated) regions amounts to propagation into an unstable state (Fisher, 1937; Kolmogorov et al., 1937; Aronson and Weinberger, 1978), a phenomenon that has generated a vast amount of literature (van Saarloos, 2003). Given the mean-field equations (A.2), the front is “pulled” by the leading edge into the unstable state. For a sufficiently sharp initial density profile (Murray, 2003), the asymptotic velocity is determined by the infinitesimally small density of invaders that intrude into the linearly unstable region dominated by the resident species. Linearizing Eqs. (A.2) about the unstable state, $\rho_1 = 1 - \mu/\alpha_1 + \phi_1$, $\rho_2 = \phi_2$, one obtains for the density of invaders

$$\frac{\partial \phi_2(\mathbf{x}, t)}{\partial t} = \frac{\mu}{4} \frac{\alpha_2}{\alpha_1} \nabla^2 \phi_2(\mathbf{x}, t) + \mu \left(\frac{\alpha_2}{\alpha_1} - 1 \right) \phi_2(\mathbf{x}, t). \quad (\text{A.3})$$

Performing standard analysis (Murray, 2003; van Saarloos, 2003) of this equation with $D \equiv (\mu/4)(\alpha_2/\alpha_1)$ and $r \equiv \mu(\alpha_2/\alpha_1 - 1)$, the effective diffusion and reaction coefficients, respectively, we obtain the asymptotic velocity of the “marginally stable” invading fronts, $v_p = 2\sqrt{Dr}$, i.e.,

$$v_p = \frac{\mu}{\alpha_1} \sqrt{\alpha_2(\alpha_2 - \alpha_1)}. \quad (\text{A.4})$$

v_p is the minimal velocity of a traveling wave permitted by Eqs. (A.2), and is actually realized by the deterministic nonlinear reaction–diffusion dynamics for sufficiently sharp initial profiles (Murray, 2003; van Saarloos, 2003). Note that we also performed the numerical iteration of the nonlinear difference equations (A.1) [the underlying natural discretization of the corresponding reaction–diffusion system (A.2)] (O'Malley et al., 2006b, 2009). The results show strong agreement with velocity of the linearized equations (A.4) [Fig. 5(b)]. Despite the nonstandard nonlinear (but deterministic) system of Eqs. (A.2), the front velocity can be fully governed by the linearized system where the front is pulled by the leading edge.

In discrete individual-based models with limited diffusion (resulting in strongly correlated front fluctuations), one does not expect Eq. (A.4) to provide a good approximation for the asymptotic front velocity (Moro, 2001, 2003). Instead, Eq. (A.4) can serve as a baseline reference for comparison with the actual front velocity. For the deterministic front just discussed, where invasion is dominated by infinitesimal densities at the leading edge, one can also obtain the width of the interfacial region (Murray, 2003;

van Saarloos, 2003), $w \simeq \sqrt{D/r} = (1/2)(1 - \alpha_1/\alpha_2)^{-1/2}$, independently of the landscape size L_y .

In passing, we consider the velocity results for our model's reaction–diffusion approximation in light of a spatial-competition model by Lewis et al. (2002). Our model assumes preemptive competition. Since resident and invader use the limiting resource so similarly (interact strongly), our model's mean-field approximation prohibits coexistence. The invader's advance translates one boundary equilibrium into another. As noted above, iterating Eqs. (A.1) produces a velocity matching the pulled-front velocity v_p predicted by the linearizing our model's reaction–diffusion approximation. That is, for all parameter combinations we evaluated, the “linear conjecture” (Mollison and Levin, 1995) predicts the mean-field velocity.

Lewis et al. (2002) write a two-species competition model of Lotka–Volterra form, with each species diffusing along a one-dimensional continuum. The spatially homogeneous equilibria are standard; coexistence is stable if self-regulation in both species is stronger than interspecific competition. The authors derive a set of sufficient conditions under which the linear conjecture will predict their model's invasion velocity. Outside parameter ranges specified by these conditions, their model's velocity might or might not match that obtained by linearizing the dynamics at the invasive front's leading edge. Put simply, they find that the linear conjecture holds when both diffusion of the competitively superior invader is not too small compared to the resident's diffusion, and the species do not interact too strongly. Our results, Fig. 5(b), are numerical; if the result for Lotka–Volterra competition with diffusion (Lewis et al., 2002) applies more generally, our mean-field approximation's velocity might or might not match v_p so closely for other parameter values. We emphasize strongly that our important results on invasion velocity concern the differences between the discrete, stochastic model's velocity (a pushed front) and that of the associated reaction–diffusion model (a pulled front), quite independently of whether or not the latter can be approximated via the linear conjecture.

Appendix B: The KPZ equation and scaling behavior of the KPZ universality class

The interface dynamics of a large class of discrete individual-based models can be described by the effective (or coarse-grained) Langevin equation (Kardar et al., 1986)

$$\frac{\partial h(y, t)}{\partial t} = v \frac{\partial^2 h(y, t)}{\partial y^2} + \lambda \left(\frac{\partial h(y, t)}{\partial y} \right)^2 + \zeta(y, t), \quad (\text{B.1})$$

where v is the effective “surface tension,” λ is the nonlinear coupling constant, and $\zeta(y, t)$ is delta-correlated Gaussian noise, $\langle \zeta(y, t) \rangle = 0$ and $\langle \zeta(y, t) \zeta(y', t') \rangle = 2\Gamma \delta(y - y') \delta(t - t')$, with Γ being the noise intensity. $\delta(\dots)$ is the Dirac delta. The coupling constants and the noise intensity depend strongly on the details of the course-graining procedure (i.e., the local rates or the finite neighborhood size in the original discrete model, and how the continuum limit was taken from that model). The variable $h(y, t)$ is the coarse-grained (or mesoscopic) limit of the local front advancements $h_y(t)$. In some cases, this procedure can be carried out explicitly from first principles (Plischke et al., 1987; Korniss et al., 2000, 2003). More often, however, due to the complexity of the details

of the model, this task is insurmountable. Even then, however, fundamental symmetry considerations can strongly motivate the applicability of the KPZ equation. Thus, equations of this sort should not be interpreted as a rigorous continuum limit derived from the local interface rules, but rather as a coarse-grained description. This approach has been enormously successful in advancing understanding of large-scale morphological properties of interfaces and surfaces in complex natural and artificial systems (Barabási and Stanley, 1995; Halpin-Healy and Zhang, 1995; Korniss et al., 2000; Brú et al., 2003). A number of models in the large-scale limit can be effectively described by Eq. (B.1), i.e., interesting attributes of these models (e.g., the width, the extreme advance, and their distributions) exhibit the same scaling behavior and shape as given by the solution of Eq. (B.1). These models are said to belong to the KPZ universality class.

B.1 Temporal and habitat-size scaling of KPZ fronts

The temporal and habitat-size scaling of the width $\langle w^2(L, t) \rangle$ typically identifies the universality class of an advancing front. In finite systems, the width grows as $\langle w^2(L, t) \rangle \sim t^{2\beta}$ from early to intermediate times. At a system-size-dependent crossover time, $t_\times \sim L^z$, it saturates (reaches steady state) and scales as $\langle w_{\text{sat}}^2 \rangle \equiv \langle w^2(L, \infty) \rangle \sim L^{2\alpha}$, where L is the transverse linear system size. α , β , and z are referred to as the roughness, growth, and dynamic exponents, respectively. The exponents obey the scaling relationship $\alpha = \beta z$. The full temporal and finite-size behavior (reproducing the growth and the steady state regimes as limiting cases) can be captured by the Family–Vicsek scaling form (Family and Vicsek, 1985)

$$\langle w^2(L, t) \rangle = L^{2\alpha} f(t/L^z). \quad (\text{B.2})$$

For small values of its argument, $f(x)$ behaves as a power law, while for large arguments it approaches a constant

$$f(x) = \begin{cases} x^{2\beta} & \text{for } x \ll 1, \\ \text{const.} & \text{for } x \gg 1, \end{cases} \quad (\text{B.3})$$

yielding the scaling behavior of the width, first in the growth regime and then in the steady-state regime [Eq. (3), Fig. 3], provided the scaling relationship $\alpha = \beta z$ holds. For the KPZ universality class, these exponents can be obtained exactly, $\alpha = 1/2$, $\beta = 1/3$, and $z = 3/2$ (Kardar et al., 1986; Barabási and Stanley, 1995). Furthermore, in the steady state, employing path-integral techniques, both the width distribution (Foltin et al., 1994) and the distribution of the extremes (Majumdar and Comtet, 2004) were obtained analytically. Scaling behaviors then can be compared to those obtained from a discrete model (e.g., by simulations), indicating whether or not the discrete stochastic model belongs to the KPZ universality class.

B.2 Steady-state width distribution of the KPZ universality class

The width distribution typically provides a strong signature of the underlying universality class of the fluctuating, growing interface (Antal et al., 2001, 2002). It is important to note that for models with local dispersal, the measured probability density (or histogram)

of the individual (row y) interface fluctuations (or “parent” densities) $P(h_y - \bar{h})$ have tails that decay faster than any power law (approximately Gaussian in our model, but this local property depends strongly on model details). We also note that if the height fluctuations $(h_y - \bar{h})^2$ in Eq. (2) were independent (or their correlation along the interface decayed sufficiently fast), the probability density of w^2 would be Gaussian, by the central limit theorem. Instead, for our roughened front, these variables are strongly correlated. As universality arguments suggest, the shape of the steady-state distribution of the width for all (sufficiently large) system sizes and for all models belonging to the KPZ class will be identical, governed by a single scale. That is, the average width $\langle w^2 \rangle \sim L$. Hence, the width distribution for any model in this class with rough fronts can be written as

$$P(w^2, L) = \frac{1}{\langle w^2 \rangle} \Phi(w^2 / \langle w^2 \rangle), \quad (\text{B.4})$$

where $\Phi(s)$ is the probability density of the scaled variable $s \equiv w^2 / \langle w^2 \rangle$. $\Phi(s)$ for periodic boundary conditions (used in our simulations) was obtained by Foltin et al. (1994), and is given by

$$\Phi(s) = \frac{\pi^2}{3} \sum_{n=1}^{\infty} (-1)^{n-1} n^2 e^{-(\pi^2/6)n^2 s}. \quad (\text{B.5})$$

The universal scaling function above can be employed to test whether a discrete individual-based invasion model with a rough front belongs to the KPZ class. Analyzing the width histograms, as empirical measures of the theoretical probability density, supports our conclusion that the two-species invasion model, the focus of our investigations, belongs to the KPZ class [Fig. B.1]. Note that no fits were used in collapsing the scaled data to the theoretical curve. Analytic scaling functions for the width distribution can also be obtained for other types of boundary conditions, e.g., “window” or free (Antal et al., 2002).

To emphasize the concept of universality, we also analyzed data and constructed histograms for propagating fronts in two well-known invasion models, the Eden model and the contact process. We note that the fronts in both of these individual-based models have long been believed to belong to the KPZ class (Jullien and Botet, 1985a, 1985b; Plischke and Rácz, 1985; Kertész and Wolf, 1988; Ferreira and Alves, 2006; Moro, 2001). The scaled probability densities exhibit progressive data collapse onto the universal scaled KPZ density [Fig. B.2], offering further support that the invasive fronts in the Eden model and in the basic contact process belong to the KPZ class.

B.3 Asymptotic velocity of KPZ fronts: temporal and habitat-size corrections

As described in the text, a model's asymptotic front velocity cannot be universal. However, Krug and Meakin (1990) showed that the forms of the temporal and finite-size ($L_y = L$) corrections are universal within a given class. Above we demonstrated that the propagating interface in our two-species invasion model belongs to the KPZ universality class with exponents $\alpha = 1/2$, $\beta = 1/3$, and $z = 3/2$. Using Krug and Meakin's result, one obtains the corrections to the front velocity $v(t, L)$,

$$v(t, L) = \begin{cases} v^* - c_1 t^{-2(1-\alpha)/z} = v^* - c_1 t^{-2/3} & \text{for } t \ll L^z, \\ v^* - c_2 L^{-2(1-\alpha)} = v^* - c_2 L^{-1} & \text{for } t \gg L^z, \end{cases} \quad (\text{B.6})$$

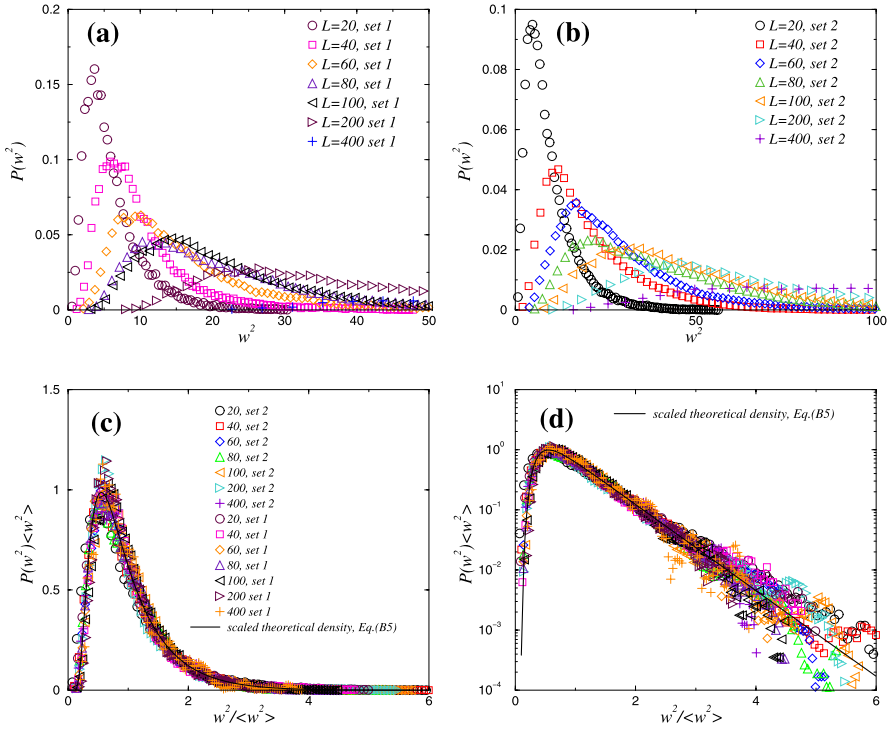


Fig. B.1 (a) Steady-state width distributions in our two-species invasive front for several habitat sizes with parameters $\alpha_1 = 0.5$, $\alpha_2 = 0.7$, $\mu = 0.2$ (“Set 1”); and (b) for $\alpha_1 = 0.7$, $\alpha_2 = 0.8$, $\mu = 0.1$ (“Set 2”). (c) Scaled histograms for all habitat sizes, for both Set 1 and Set 2. The solid curve is the scaled analytic width distribution of the KPZ class, Eq. (B.5) (Foltin et al., 1994). (d) Same scaled data as in (c), but on lin-log scales.

where c_1 and c_2 are non-universal constants that depend, as does v^* , on propagation and mortality rates at the level of individual competitors.

The first expression in Eqs. (B.6) indicates that the early temporal correction to the front’s velocity scales as $\mathcal{O}(t^{-2/3})$. Pulled fronts produced in deterministic reaction–diffusion models exhibit $\mathcal{O}(t^{-1})$ corrections to the asymptotic velocity (Andow et al., 1990; Holmes et al., 1994). A discrete model’s pushed front has a larger temporal correction; effects of time since initiation of invasion (from $t = 0$ until $t_x \sim L^z$) persist longer in the stochastic case. In the simulations, we measure $\bar{h}(t)/t$ as it follows the same temporal and system-size scaling as those of $v(t, L)$ [Eq. (B.6)] (O’Malley et al., 2006b). Figure B.3(a) supports the above scaling for our discrete individual-based two-species invasion front.

More importantly, the second expression in Eq. (B.6) predicts that after roughening equilibrates, the invading species’ velocity must be corrected according to the size of the habitat invaded. This correction scales as $\mathcal{O}(L^{-1})$. Steady-state velocity increases with habitat size; longer invading fronts move faster. Figure B.3(b) and its inset show how this asymptotic behavior is controlled by system size L . Observed corrections to the ve-

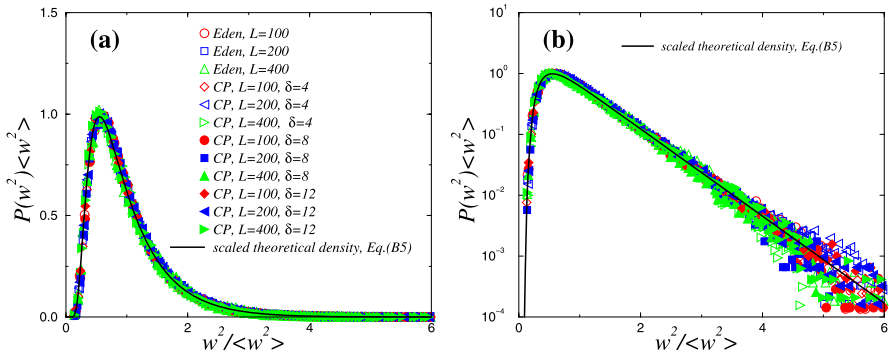


Fig. B.2 (a) Scaled steady-state width distributions for the contact process (CP) and for the Eden model for $L = 100, 200, 400$. For both models, there is only one species present (invaders) with local propagation rate α_2 and mortality rate μ . For the CP, we set $\alpha_2 = 1$ and $\mu = 0.20$. The front dynamics of the CP for $\alpha_2 = 1$ and $\mu = 0$ is equivalent to a variant of the Eden model (Jullien and Botet, 1985a), and we used these parameter values to obtain the Eden data. For the Eden model, we used only nearest-neighbor propagation ($\delta = 4$). For the CP, we also explored different neighborhood sizes, $\delta = 4, 8, 12$; all are shown on the plot. The solid curve is the scaled analytic KPZ width distribution, Eq. (B.5) (Foltin et al., 1994). (b) Same scaled data as in (a) but on lin-log scales.

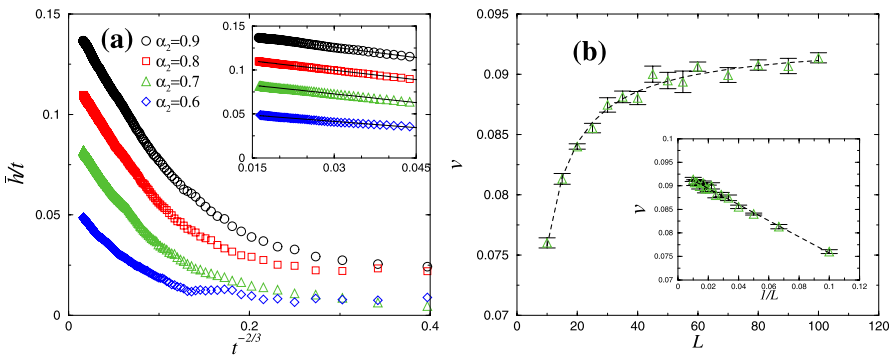


Fig. B.3 (a) Temporal corrections to the asymptotic front velocity for $L = 800$ for different values of α_2 , with $\alpha_1 = 0.50$ and $\mu = 0.20$. The horizontal (time) axis is scaled as $t^{-2/3}$, motivated by the form of the corrections of the one-dimensional KPZ class [Eq. (B.6)]. The inset enlarges the region of (a) where the universal temporal corrections follow the KPZ behavior. The straight solid lines correspond to the linear scaling as a function of $t^{-2/3}$. (b) Finite-size corrections to the asymptotic velocity as a function of L^{-1} , motivated by the universal corrections of the one-dimensional KPZ class, for $\alpha_1 = 0.50, \alpha_2 = 0.70$, and $\mu = 0.20$. The straight dashed line corresponds to the linear behavior as a function of $1/L$.

locity v^* decline linearly as a function of L^{-1} , in accordance with the second expression Eq. (B.6). The physical theory for roughened interfaces explains the effect of habitat size on frontal velocity, and further gives the form of the quantitative dependence. These corrections to the steady-state velocity were observed qualitatively for the basic contact process (Ellner et al., 1998) and for the Eden model (Kawasaki et al., 2006), but neither

study addressed either the quantitative correction for habitat (system) size or the underlying basis for the dynamic behavior: KPZ roughening of the front.

B.4 Distribution of extremes in steady-state KPZ fronts: the Airy density

The distribution of the front's extreme advance (relative to the mean) provides an additional strong signature of the underlying universality class of a stochastic interface. This distribution was only recently obtained in analytic form (Majumdar and Comtet, 2004, 2005).

As universality arguments imply (Schehr and Majumdar, 2006), the shape of the steady-state distribution of the front's extreme advance (relative to the mean) for all (sufficiently large) system sizes and for all models belonging to the KPZ class will be identical, governed by a single scale, $\langle \Delta_{\max} \rangle \sim L^{1/2}$. For a given model with a rough front one has

$$P(\Delta_{\max}, L) = \frac{1}{\langle \Delta_{\max} \rangle} \Psi(\Delta_{\max}/\langle \Delta_{\max} \rangle), \quad (\text{B.7})$$

where $\Psi(u)$ is the probability density of the scaled variable $u \equiv \Delta_{\max}/\langle \Delta_{\max} \rangle$. For periodic boundary conditions (employed in our simulations), Majumdar and Comtet (2004, 2005) obtained the analytic result

$$\Psi(u) = \sqrt{\frac{\pi}{8}} f_A \left(\sqrt{\frac{\pi}{8}} u \right), \quad (\text{B.8})$$

where f_A is the Airy density function. A continuous random variable X ($X > 0$) has an Airy probability density if:

$$f_A(X) = \frac{2\sqrt{6}}{X^{10/3}} \sum_{k=1}^{\infty} e^{-b_k/X^2} b_k^{2/3} U(-5/6, 4/3, b_k/X^2), \quad (\text{B.9})$$

where $b_k = 2a_k^3/27$, and $U(\cdot, \cdot, \cdot)$ is the confluent hypergeometric function. a_k is the magnitude of the k -th root of the Airy function $Ai(\cdot)$ on the negative real axis (Abramowitz and Stegun, 1972). The Airy distribution arises in a remarkable number of different applications, including the extremum of a set of correlated random variables; see Majumdar and Comtet (2005), Schehr and Majumdar (2006), and Guclu et al. (2007).

References

- Abramowitz, M., Stegun, I.A., 1972. Handbook of Mathematical Functions. National Bureau of Standards, Washington.
- Allstadt, A., Caraco, T., Korniss, G., 2007. Ecological invasion: spatial clustering and the critical radius. *Evol. Ecol. Res.* 9, 1–20.
- Andow, D.A., Kareiva, P.M., Levin, S.A., Okubo, A., 1990. Spread of invading organisms. *Landsc. Ecol.* 4, 177–188.
- Antal, T., Droz, M., Györgyi, G., Rácz, Z., 2001. $1/f$ noise and extreme value statistics. *Phys. Rev. Lett.* 87, 240601. 4p.
- Antal, T., Droz, M., Györgyi, G., Rácz, Z., 2002. Roughness distribution of $1/f^\alpha$ signals. *Phys. Rev. E* 65, 046140. 12p.

- Antonovics, J., McKane, A.J., Newman, T.J., 2006. Spatiotemporal dynamics in marginal populations. *Am. Nat.* 167, 16–27.
- Aronson, D.G., Weinberger, H.F., 1978. Multidimensional nonlinear diffusion arising in population genetics. *Adv. Math.* 30, 33–76.
- Aylor, D.E., 2003. Spread of plant disease on a continental scale: role of aerial dispersal of pathogens. *Ecology* 84, 1989–1997.
- Barabási, A.-L., Stanley, H.E., 1995. *Fractal Concepts in Surface Growth*. Cambridge University Press, Cambridge.
- ben-Avraham, D., 1998. Fisher waves in the diffusion limited coalescence process. *Phys. Lett. A* 247, 53–58.
- Berman, S.M., 1964. Limit theorems for the maximum term in stationary sequences. *Ann. Math. Stat.* 35, 502–516.
- Bjornstad, O.N., Peltonin, M., Liebhold, A.M., Baltensweiler, W., 2002. Waves of larch budmoth outbreaks in the European Alps. *Science* 298, 1020–1023.
- Blythe, R.A., Evans, M.R., 2001. Slow crossover to Kardar–Parisi–Zhang scaling. *Phys. Rev. E* 64, 051101, 5 p.
- Brú, A., Albertos, S., Subiza, J.L., García-Asenjo, J.L., Brú, I., 2003. The universal dynamics of tumor growth. *Biophys. J.* 85, 2948–2961.
- Cain, M.L., Pacala, S.W., Silander, J.A. Jr., Fortin, M.-J., 1995. Neighborhood models of clonal growth in the white clover *Trifolium repens*. *Am. Nat.* 145, 888–917.
- Cannas, S.A., Marco, D.E., Montemurro, M.A., 2006. Long range dispersal and spatial pattern formation in biological invasions. *Math. Biosci.* 203, 155–170.
- Cantrell, R.S., Cosner, C., 1991. The effect of spatial heterogeneity in population dynamics. *J. Math. Biol.* 29, 315–338.
- Caraco, T., Glavanakov, S., Chen, G., Flaherty, J.E., Ohsumi, T.K., Szymanski, B.K., 2002. Stage-structured infection transmission and a spatial epidemic: a model for Lyme disease. *Am. Nat.* 160, 348–359.
- Cardy, J., 1996. *Scaling and Renormalization in Statistical Physics*. Cambridge University Press, Cambridge.
- Clark, J.S., Fastie, C., Hurr, G., Jackson, S.T., Johnson, C., King, G.A., Lewis, M., Lynch, J., Pacala, S., Prentice, C., Schupp, E.W., Webb, T., III, Wyckoff, P., 1998. Reid's paradox of rapid plant migration. *BioScience* 48, 13–24.
- Clark, J.S., Lewis, M., Horvath, L., 2001. Invasion by extremes: population spread with variation in dispersal and reproduction. *Am. Nat.* 157, 537–554.
- Clark, J.S., Lewis, M., McLachlan, J.S., HilleRisLambers, J., 2003. Estimating population spread: what can we forecast and how well? *Ecology* 84, 1979–1988.
- Comins, H.N., Noble, I.R., 1985. Dispersal, variability, and transient niches: species coexistence in a uniformly variable environment. *Am. Nat.* 126, 706–723.
- Connolly, S.R., Moko, S., 2003. Space preemption, size-dependent competition and the coexistence of clonal growth forms. *Ecology* 84, 2979–2988.
- D'Antonio, C.M., 1993. Mechanisms controlling invasion of coastal plant communities by the alien succulent *Carpobrotus edulis*. *Ecology* 74, 83–95.
- DeAngelis, D.L., Gross, L.J. (Eds.), 1992. *Individual-Based Models and Approaches in Ecology*. Routledge, Chapman and Hall, New York.
- Doering, C.R., Mueller, C., Smereka, P., 2003. Interacting particles, the stochastic Fisher–Kolmogorov–Petrovsky–Piscounov equation, and duality. *Physica A* 325, 243–259.
- Doi, M., 1976. Stochastic theory of diffusion-controlled reaction. *J. Phys. A* 9, 1479–1495.
- Durrett, R., Levin, S.A., 1994a. Stochastic spatial models: a user's guide to ecological applications. *Philos. Trans. R. Soc. Lond. B* 343, 329–350.
- Durrett, R., Levin, S.A., 1994b. The importance of being discrete (and spatial). *Theor. Popul. Biol.* 46, 363–394.
- Dwyer, G., 1992. On the spatial spread of insect pathogens: theory and experiment. *Ecology* 73, 479–494.
- Dwyer, G., Elkinton, S., 1995. Host dispersal and the spatial spread of insect pathogens. *Ecology* 76, 1262–1275.
- Dwyer, G., Morris, W.F., 2006. Resource-dependent dispersal and the speed of biological invasions. *Am. Nat.* 167, 165–176.
- Eden, M., 1961. A two-dimensional growth process. In: Neyman, J. (Ed.), 4th Berkeley Symposium on Mathematical Statistics and Probability, vol. 4, pp. 223–239. University of California Press, Berkeley.

- Ellner, S.P., Sasaki, A., Haraguchi, Y., Matsuda, H., 1998. Speed of invasion in lattice population models: pair-edge approximation. *J. Math. Biol.* 36, 469–484.
- Elton, C.S., 1958. *The Ecology of Invasions by Animals and Plants*. Methuen, London.
- Escudero, C., Buceta, J., de la Rubia, F.J., Lindenberg, K., 2004. Extinction in population dynamics. *Phys. Rev. E* 69, 021908, 9 p.
- Family, F., Vicsek, T., 1985. Scaling of the active zone in the Eden process on percolation networks and the ballistic deposition model. *J. Phys. A* 18, L75–L81.
- Ferrandino, F.J., 1996. Length scale of disease spread: fact or artifact of experimental geometry? *Phytopathology* 86, 806–811.
- Ferreira, S.C. Jr., Alves, S.G., 2006. Pitfalls in the determination of the universality class of radial clusters. *J. Stat. Mech.* 11, P11007, 11 p.
- Fisher, M.C., Koenig, G.L., White, T.J., Sans-Blas, G., Negroni, R., Alvarez, I.G., Wanke, B., Taylor, J.W., 2001. Biogeographic range expansion into South America by *Coccidioides immitis* mirrors New World patterns of human migration. *Proc. Nat. Acad. Sci. USA* 98, 4558–4562.
- Fisher, R.A., 1937. The wave of advance of advantageous genes. *Ann. Eugen. Lond.* 7, 355–369.
- Fisher, R.A., Tippett, L.H.C., 1928. The frequency distribution of the largest or smallest member of a sample. *Proc. Camb. Philos. Soc.* 24, 180–191.
- Foltin, G., Oerding, K., Rácz, Z., Workman, R.L., Zia, R.K.P., 1994. Width distribution for random-walk interfaces. *Phys. Rev. E* 50, R639–R642.
- Frantzen, J., van den Bosch, F., 2000. Spread of organisms: can travelling and dispersive waves be distinguished? *Basic Appl. Ecol.* 1, 83–91.
- Galambos, J., 1987. *The Asymptotic Theory of Extreme Order Statistics*, 2nd edn. Krieger Publishing, Malabar.
- Galambos, J., Lechner, J., Simin, E. (Eds.), 1994. *Extreme Value Theory and Applications*. Kluwer, Dordrecht.
- Gandhi, A., Levin, S., Orszag, S., 1999. Nucleation and relaxation from meta-stability in spatial ecological models. *J. Theor. Biol.* 200, 121–146.
- Gardiner, C.W., 1985. *Handbook of Stochastic Methods for Physics, Chemistry and the Natural Sciences*, 2nd edn. Springer, Berlin.
- Guclu, H., Korniss, G., 2004. Extreme fluctuations in small-worlds with relaxational dynamics. *Phys. Rev. E* 69, 065104(R), 4 p.
- Guclu, H., Korniss, G., Toroczkai, Z., 2007. Extreme fluctuations in noisy task-completion landscapes on scale-free networks. *Chaos* 17, 026104, 13 p.
- Gumbel, E.J., 1958. *Statistics of Extremes*. Columbia University Press, New York.
- Halpin-Healy, T., Zhang, Y.-C., 1995. Kinetic roughening phenomena, stochastic growth, directed polymers and all that. Aspects of multidisciplinary statistical mechanics. *Phys. Rep.* 254, 215–414.
- Harris, T.E., 1974. Contact interaction on a lattice. *Ann. Probab.* 2, 969–988.
- Hastings, A., Cuddington, K., Davies, K.F., Dugaw, C.J., Elmendorf, S., Freestone, A., Harrison, S., Holland, M., Lambrinos, J., Malvadkar, U., Melbourne, B.A., Moore, K., Taylor, C., Thomson, D., 2005. The spatial spread of invasions: new developments in theory and evidence. *Ecol. Lett.* 8, 91–101.
- Hinrichsen, H., 2000. Non-equilibrium critical phenomena and phase transitions into absorbing states. *Adv. Phys.* 49, 815–958.
- Holmes, E.E., Lewis, M.A., Banks, J.E., Veit, R.R., 1994. Partial differential equations in ecology: spatial interactions and population dynamics. *Ecology* 75, 17–29.
- Holway, D.A., 1998. Factors governing rate of invasion: a natural experiment using Argentine ants. *Oecologia* 115, 206–212.
- Hoopes, M.F., Hall, L.M., 2002. Edaphic factors and competition affect pattern formation and invasion in a California grassland. *Ecol. Appl.* 12, 24–39.
- Hosono, Y., 1998. The minimal speed of travelling fronts for a diffusive Lotka-Volterra competition model. *Bull. Math. Biol.* 60, 435–448.
- Jullien, R., Botet, R., 1985a. Surface thickness in the Eden model. *Phys. Rev. Lett.* 54, 2055.
- Jullien, R., Botet, R., 1985b. Scaling properties of the surface of the Eden model. *J. Phys. A* 18, 2279–2287.
- Kardar, M., Parisi, G., Zhang, Y.-C., 1986. Dynamic scaling of growing interfaces. *Phys. Rev. Lett.* 56, 889–892.
- Kawasaki, K., Takasu, F., Caswell, H., Shigesada, N., 2006. How does stochasticity in colonization accelerate the speed of invasion in a cellular automaton model? *Ecol. Res.* 21, 334–345.
- Kertész, J., Wolf, D.E., 1988. Noise reduction in Eden models: II. Surface structure and intrinsic width. *J. Phys. A, Math. Gen.* 21, 747–761.

- Kolmogorov, A., Petrovsky, N., Piskounov, N.S., 1937. A study of the equation of diffusion with increase in the quantity of matter, and its application to a biological problem. *Mosc. Univ. Bull. Math.* 1, 1–25.
- Korniss, G., Caraco, T., 2005. Spatial dynamics of invasion: the geometry of introduced species. *J. Theor. Biol.* 233, 137–150.
- Korniss, G., Schmittmann, B., 1997. Structure factors and their distributions in driven two-species models. *Phys. Rev. E* 56, 4072–4084.
- Korniss, G., Toroczkai, Z., Novotny, M.A., Rikvold, P.A., 2000. From massively parallel algorithms and fluctuating time horizons to nonequilibrium surface growth. *Phys. Rev. Lett.* 84, 1351–1354.
- Korniss, G., Novotny, M.A., Guclu, H., Toroczkai, Z., Rikvold, P.A., 2003. Suppressing roughness of virtual times in parallel discrete-event simulations. *Science* 299, 677–679.
- Kot, M., Lewis, M.A., van den Driessche, P., 1996. Dispersal data and the spread of invading organisms. *Ecology* 77, 2027–2042.
- Krug, J., Meakin, P., 1990. Universal finite-size effects in the rate of growth processes. *J. Phys. A* 23, L987–L994.
- Lewis, M.A., 1997. Variability, patchiness, and jump dispersal in the spread of an invading population. In: Tilman, D., Kareiva, P. (Eds.), *Spatial Ecology: The Role of Space in Population Dynamics and Interspecific Interactions*, pp. 46–69. Princeton University Press, Princeton.
- Lewis, M.A., 2000. Spread rate for a nonlinear stochastic invasion. *J. Math. Biol.* 41, 430–454.
- Lewis, M.A., Li, B., Weinberger, H.F., 2002. Spreading speed and linear determinacy for two-species competition models. *J. Math. Biol.* 45, 219–233.
- Lockwood, J.L., Hoopes, M.F., Marchetti, M., 2007. *Invasion Ecology*. Blackwell, Malden.
- Majumdar, S.N., Comtet, A., 2004. Exact maximal height distribution of fluctuation interfaces. *Phys. Rev. Lett.* 92, 225501, 4 p.
- Majumdar, S.N., Comtet, A., 2005. Airy distribution function: from the area under a Brownian excursion to the maximal height of fluctuating interfaces. *J. Stat. Phys.* 119, 776–826.
- McKane, A.J., Newman, T.J., 2004. Stochastic models in population biology and their deterministic analogues. *Phys. Rev. E* 70, 041902, 19 p.
- Minogue, K.P., Fry, W.E., 1983. Models for the spread of plant disease: some experimental results. *Phytopathology* 73, 1173–1176.
- Mollison, D., Levin, S.A., 1995. Spatial dynamics of parasitism. In: Grenfell, B.T., Dobson, A.P. (Eds.), *Ecology of Infectious Diseases in Natural Populations*, pp. 384–398. Cambridge University Press, Cambridge.
- Moro, E., 2001. Internal fluctuations effects on Fisher waves. *Phys. Rev. Lett.* 87, 238303, 4 p.
- Moro, E., 2003. Emergence of pulled fronts in fermionic microscopic particle models. *Phys. Rev. E* 68, 025102, 4 p.
- Murray, J.D., 2003. *Mathematical Biology*, vol. 2. Springer, New York.
- Nash, D.R., Agassiz, D.J.L., Godfray, H.C.J., Lawton, J.H., 1995. The pattern of spread of invading species: two leaf-mining moths colonizing Great Britain. *J. Anim. Ecol.* 64, 225–233.
- Neubert, M.G., Caswell, H., 2000. Demography and dispersal: calculation and sensitivity analysis of invasion speed for structured populations. *Ecology* 81, 1613–1628.
- Oborny, B., Meszéna, G., Szabó, G., 2005. Dynamics of populations on the verge of extinction. *Oikos* 109, 291–296.
- O'Malley, L., Allstadt, A., Korniss, G., Caraco, T., 2005. Nucleation and global time scales in ecological invasion under preemptive competition. In: Stocks, N.G., Abbott, D., Morse, R.P. (Eds.), *Fluctuations and Noise in Biological, Biophysical, and Biomedical Systems III*, pp. 117–124. SPIE, Pullman.
- O'Malley, L., Basham, J., Yasi, J.A., Korniss, G., Allstadt, A., Caraco, T., 2006a. Invasive advance of an advantageous mutation: nucleation theory. *Theor. Popul. Biol.* 70, 464–478.
- O'Malley, L., Kozma, B., Korniss, G., Rácz, Z., Caraco, T., 2006b. Fisher waves and front propagation in a two-species invasion model with preemptive competition. *Phys. Rev. E* 74, 041116, 7 p.
- O'Malley, L., Kozma, B., Korniss, G., Rácz, Z., Caraco, T., 2009. Fisher waves and the velocity of front propagation in a two-species invasion model with preemptive competition. In: Landau, D.P., Lewis, S.P., Schüttler, H.-B. (Eds.), *Computer Simulation Studies in Condensed Matter Physics XIX*, Springer Proceedings in Physics, vol. 123, pp. 73–78. Springer, Heidelberg.
- Parker, I.M., Reichard, S.H., 1998. Critical issues in invasion biology for conservation science. In: Fieldler, P.L., Kareiva, P.M. (Eds.), *Conservation Biology*, 2nd edn., pp. 283–305. Chapman and Hall, New York.
- Pechenik, L., Levine, H., 1999. Interfacial velocity corrections due to multiplicative noise. *Phys. Rev. E* 59, 3893–3900.

- Peliti, L., 1985. Path integral approach to birth-death processes on a lattice. *J. Phys. (Paris)* 46, 1469–1483.
- Pimentel, D., Lach, L., Zuniga, R., Morrison, D., 2000. Environmental and economic costs of nonindigenous species in the United States. *Bioscience* 50, 53–65.
- Plischke, M., Rácz, Z., 1985. Dynamic scaling and the surface structure of Eden clusters. *Phys. Rev. A* 32, 3825–3828.
- Plischke, M., Rácz, Z., Liu, D., 1987. Time-reversal invariance and universality of two-dimensional growth models. *Phys. Rev. B* 35, 3485–3495.
- Rácz, Z., Gálfi, L., 1988. Properties of the reaction front in an $A + B \rightarrow C$ type reaction–diffusion process. *Phys. Rev. A* 38, 3151–3154.
- Raychaudhuri, S., Cranston, M., Przybyla, C., Shapir, Y., 2001. Maximal height scaling of kinetically growing surfaces. *Phys. Rev. Lett.* 87, 136101, 4 p.
- Rosenzweig, M.L., 2001. The four questions: what does the introduction of exotic species do to diversity? *Evol. Ecol. Res.* 3, 361–371.
- Ruesink, J.L., Parker, I.M., Groom, M.J., Kareiva, P.M., 1995. Reducing the risks of nonindigenous introductions: guilty until proven innocent. *BioScience* 45, 465–477.
- Ruiz, G.M., Rawlings, T.K., Dobbs, F.C., Huq, A., Colwell, R., 2000. Global spread of microorganisms by ships. *Nature* 408, 49.
- Schehr, G., Majumdar, S.N., 2006. Universal asymptotic statistics of a maximal relative height in one-dimensional solid-on-solid models. *Phys. Rev. E* 73, 056103, 10 p.
- Schmittmann, B., Zia, R.K.P., 1995. *Statistical Mechanics of Driven Diffusive Systems. Phase Transitions and Critical Phenomena*, vol. 17. Academic Press, New York.
- Schwinning, S., Parsons, A.J., 1996. A spatially explicit population model of stoloniferous N-fixing legumes in mixed pasture with grass. *J. Ecol.* 84, 815–826.
- Shigesada, N., Kawasaki, K., 1997. *Biological Invasions: Theory and Practice*. Oxford University Press, Oxford.
- Shigesada, N., Kawasaki, K., Takeda, Y., 1995. Modeling stratified diffusion in biological invasions. *Am. Nat.* 146, 229–251.
- Silvertown, J., Lines, C.E.M., Dale, M.P., 1994. Spatial competition between grasses—rates of mutual invasion between four species and the interaction with grazing. *J. Ecol.* 82, 31–38.
- Simberloff, D., Reiva, M.A., Nuñez, M., 2002. Gringos en el bosque: introduced tree invasion in a native *Nothofagus/Austrocedrus* forest. *Biol. Invasions* 4, 35–53.
- Snyder, R.E., 2003. How demographic stochasticity can slow biological invasions. *Ecology* 84, 1333–1339.
- Tainaka, K., Kushida, M., Itoh, Y., Yoshimura, J., 2004. Interspecific segregation in a lattice ecosystem with intraspecific competition. *J. Phys. Soc. Jpn.* 73, 2914–2915.
- Thomson, N.A., Ellner, S.P., 2003. Pair-edge approximation for heterogeneous lattice population models. *Theor. Popul. Biol.* 64, 270–280.
- van Baalen, M., Rand, D.A., 1998. The unit of selection in viscous populations and the evolution of altruism. *J. Theor. Biol.* 193, 631–648.
- van den Bosch, F., Hengeveld, R., Metz, J.A.J., 1992. Analysing the velocity of animal range expansion. *J. Biogeogr.* 19, 135–150.
- van Kampen, N.G., 1976. The expansion of the master equation. *Adv. Chem. Phys.* 34, 245–309.
- van Kampen, N.G., 1981. *Stochastic Processes in Physics and Chemistry*. Elsevier, Amsterdam.
- van Saarloos, W., 2003. Front propagation into unstable states. *Phys. Rep.* 386, 29–222.
- Weinberger, H.F., Lewis, M.A., Li, B.T., 2002. Analysis of linear determinacy for spread in cooperative models. *J. Math. Biol.* 45, 183–218.
- Wilson, W., 1998. Resolving discrepancies between deterministic population models and individual-based simulations. *Am. Nat.* 151, 116–134.
- Wilson, W., de Roos, A.M., McCauley, E., 1993. Spatial instabilities within the diffusive Lotka–Volterra system: individual-based simulation results. *Theor. Popul. Biol.* 43, 91–127.
- Yasi, J., Korniss, G., Caraco, T., 2006. Invasive allele spread under preemptive competition. In: Landau, D.P., Lewis, S.P., Schüttler, H.-B. (Eds.), *Computer Simulation Studies in Condensed Matter Physics XVIII*, Springer Proceedings in Physics, vol. 105, pp. 165–169. Springer, Heidelberg.
- Yurkonis, K.A., Meiners, S.J., 2004. Invasion impacts local species turnover in a successional system. *Ecol. Lett.* 4, 764–769.